NGU Report 2002.016

Rock avalanches, gravitational bedrock fractures and neotectonic faults onshore northern West Norway: Examples, regional distribution and triggering mechanisms

Geological Survey of Norway
N-7441 Trondheim, Norway
Tel.: 47 73 90 40 00
Telefax 47 73 92 16 20

REPORT

Report no.: 2002.016 | ISSN 0800-3416 | Grading: Open

Title:
Rock avalanches, gravitational bedrock fractures and neotectonic faults onshore northern West Norway:
Examples, regional distribution and triggering mechanisms

Authors:
Lars Harald Blikra, Alvar Braathen, Einar Anda, Knut Stalsberg and Oddvar Longva

Client:
NGU, Norsk Hydro ASA, County Council of Møre & Romsdal, County Council of Sogn & Fjordane, National fund for natural damage

County:
Møre & Romsdal and Sogn & Fjordane

Commune:

Map-sheet name (M=1:250.000)

Map-sheet no. and -name (M=1:50.000)

Deposit name and grid-reference:

Number of pages: 48 Price (NOK):
Map enclosures:

Fieldwork carried out: 1995-2001

Date of report: 23.04 2002

Project no.: 2931.00, 2689.00 and 2689.01

Person responsible: Astrid Lysså

Summary:
The present report aims on gravitational slope failures in Møre & Romsdal and Sogn & Fjordane counties. It presents selected examples and an overview of the regional occurrence of rock avalanches and other bedrock failures. The data discussed here have been collected through several NGU projects since 1995, the present one being: "Regional landslide occurrences and possible post-glacial earthquake activity in northwestern Norway" (phase D); a project funded by Norsk Hydro ASA and NGU. Geological studies show that several areas in western Norway have been affected by a significant number of large rock avalanches throughout the postglacial period. The geographic distribution of rock avalanches and gravitational bedrock fractures clearly shows a clustering in specific zones, with the highest frequency in the inner fjord areas of western Norway. The highest number of such features is found in the Romsdalen and Tafjord areas in Møre og Romsdal. Groups of rock avalanches and gravitational bedrock fractures are also found in two smaller areas of Møre & Romsdal, in a more coastal position around Oterøya and Syvdsfjorden. A group of gravitational failures also occur in the phyllite areas in Aurland, Sogn og Fjordane.

The age of the features is still poorly constrained, but a review of existing data shed som light on the time-frame. The bedrock fractures and rock avalanches around Oterøya probably occurred shortly after the deglaciation. The time constraint is weak for the coastal area further southwest, but the data point to several events of different ages. Several dated events in the inner fjord areas of Møre & Romsdal suggests high rock-avalanche activity during the second half of the Holocene. This can be seen in context with a neotectonic fault (Berill fault) in Innfjorden, west of Romsdalen. The Berill fault is at least younger than the Younger Dryas period (<11500 cal. BP). Some dates of rock avalanches around 3000 cal. BP in Innfjorden and Tafjorden indicate a relationship with the faulting event. The data from Aurland in Sogn & Fjordane suggest that the gravitational failures in the phyllite area are related to two stages, one shortly after the deglaciation and a smaller event at about 3000 cal. BP.

Review of historical earthquakes indicate that the triggering of large rock avalanches and deep-seated bedrock failures requires a minimum earthquake magnitude of about 6.0 – 6.5 on the Richter scale. The distinct clustering of features in specific zones indicates that large earthquake played a role. The recently detected neotectonic fault (Berill fault) further help to explain some rock avalanches in the fjords of Møre & Romsdal. The fault is situated in the area of the highest land-uplift gradient in western Norway, which could be the cause for crustal instability. Earthquakes related to this fault were probably of the order of M 6.5. The spatial distribution of the clustering in Møre & Romsdal seems to fit a relationship between aerial extent of landslides and earthquake magnitudes of M 6.5. In conclusion, future work should especially aim on further investigations of possible neotectonic faults, in order to get a better understanding of the palaeoseismic activity.

Keywords: Geology	Rock avalanches	Faults
Fractures	Earthquakes	Neotectonic
Hazard		

CONTENTS

1. Introduction

The data presented here have been collected through several NGU projects since 1995, and include both studies of past rock avalanches and detailed studies of potential source areas for such events. Geological mapping and studies of rock avalanches and other gravitational-slope failures are parts of NGU-projects in the Troms, Møre & Romsdal and Sogn & Fjordane counties (Blikra & Anda, 1997; Blikra *et al*. 1999; Blikra *et al*., 200B; Blikra *et al*., 2002). In addition, several smaller projects have involved such studies (e.g. Blikra *et al*., 2001), and besides, the NEONOR project partly focussed on the possible relationship between avalanching and palaeoseismic activity (Blikra 1999; Anda *et al*. 2000; Blikra & Longva 2000, Blikra *et al*., 2000A, C). This report is part of the project "Regional landslide occurrences and possible post-glacial earthquake activity in northwestern Norway" (phase D), a project funded by Norsk Hydro ASA and NGU.

Present consensus of the effects of historical earthquakes shows that many of these trigger different types of debris and rock failures (Keefer 1984; Jibson 1994). The spatial occurrence and dating of individual events can thus be used for palaeoseismic analysis. The review made by Jibson (1994) indicates that the triggering of large rock avalanches requires a minimum earthquake of about magnitude 6.0 on the Richter scale, and besides, large rock avalanches are the type of mass movement with the greatest potential in palaeoseismic studies. The present report presents selected examples and an overview of the regional occurrence of gravitational-slope failures in Møre & Romsdal and Sogn & Fjordane.

The data presented in this report has been collected during fieldwork by the following persons: Lars H. Blikra (NGU), Oddvar Longva (NGU), Alvar Braathen (NGU), Knut Stalsberg (NGU), Reidulv Bøe (NGU), Asbjørn Rune Aa (HSF), Stein Bondevik (UiT), Wojtek Nemec (UiB) and Øystein Lohne (UiB).

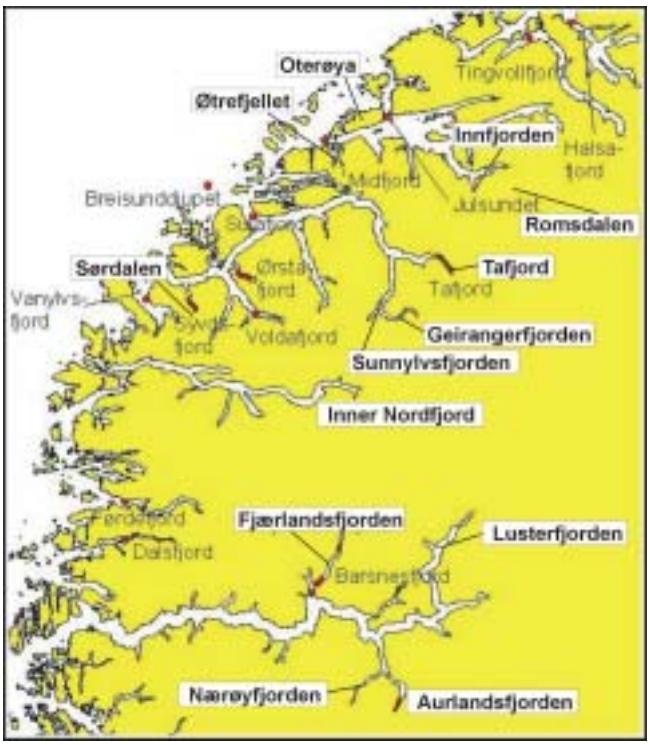

Figure. 1. Locality map showing the studied areas and other locality names used in the text.

2. Methods

Rock-avalanche deposits have been registered in Møre & Romsdal and Sogn & Fjordane counties. Many of these have been visited in the field in order to document special features, while some have undergone detailed investigations in the form of geological mapping, georadar profiling, refraction-seismic profiling and excavations (Blikra *et al*., 1999, Elvebakk & Blikra, 1999; Mauring *et al*. 1997, 1998). In addition, some of the areas characterised by extensive gravitational faulting have also undergone detailed structural mapping.

As part of the project on rock-avalanche hazard, several fjords have been covered by swath bathymetri. Most of the fjords affected by large rock avalanches are covered by reflection-seismic profiles.

Excavations in rock-avalanche deposits on land have been carried out to try to date individual mass-movement events. Results from Romsdalen and Innfjorden are presented here. Furthermore, two constrained ages are from Tafjorden, and one from Aurlandsfjorden (documented in Lepland *et al*., 2002).

NGU is cooperating with Astor Furseth from Norddal in Møre & Romsdal, who has worked on historical avalanches, and written a book on the Tafjord accident in 1934 (Furseth, 1985). We have now established a database covering more than 1100 avalanches, including numerous large rock-avalanche events. These data are also presented in this report.

3. Rock avalanches and gravitational faults/fractures: selected examples

3.1 Inner fjord areas of Møre & Romsdal

3.1.1 Romsdalen

One of the largest concentrations of rock avalanches on land is found in Romsdalen (Fig. 1), where more than 15 large rock avalanches cover almost the entire valley floor over a distance of 25 km. (Figs. 2 and 5). Debrisflow deposits, normally less than 1 m thick, are commonly found outside the bouldery rock-avalanche deposits. These debrisflows seem to have been generated by the rock-avalanche impact on the valley floor (Fig. 3). One example is found from the toe of a large rock avalanche at Venje in Romsdalen (Fig. 4), which stretches across the entire valley. Charcoal below the avalanche deposits has been radiocarbon dated, yielding ages of 1992-1882 and 1413-1352 cal. years BP. Furthermore, charcoal proves that this event occurred onshore. The elevation of the deposits, only 10 meters above the present sea level, thereby indicates a young age. Several rock-avalanche deposits in Romsdalen are situated below the marine limit and are not disturbed by fluvial erosion or marine sedimentation, showing that they were formed on land. The position of the rock-avalanche deposits are compared with the sea-level curve for the area, showing that several of them are younger than 5000 years.

Several mountain slopes with significant instability and faulting have been observed in this region. One of the largest is on the western side of Romsdalen (Figs. 5-8), which can be followed for more than 2 km. Typical deformation features include more than 20 m deep crevasses, demonstrating considerable horizontal displacement (Figs. 6 and 8). Several rock avalanches triggered from this area are deposited in the Romsdalen valley (Fig. 5). The largest has nearly crossed the valley and formed distinct concentric ridges by deforming the

underlying valley-fill sediments. A radiocarbon date in peat above this deposit gave an age of 5919-5763 cal. years BP (5118 ± 43 ^{14}C years BP), which is a minimum age of the event.

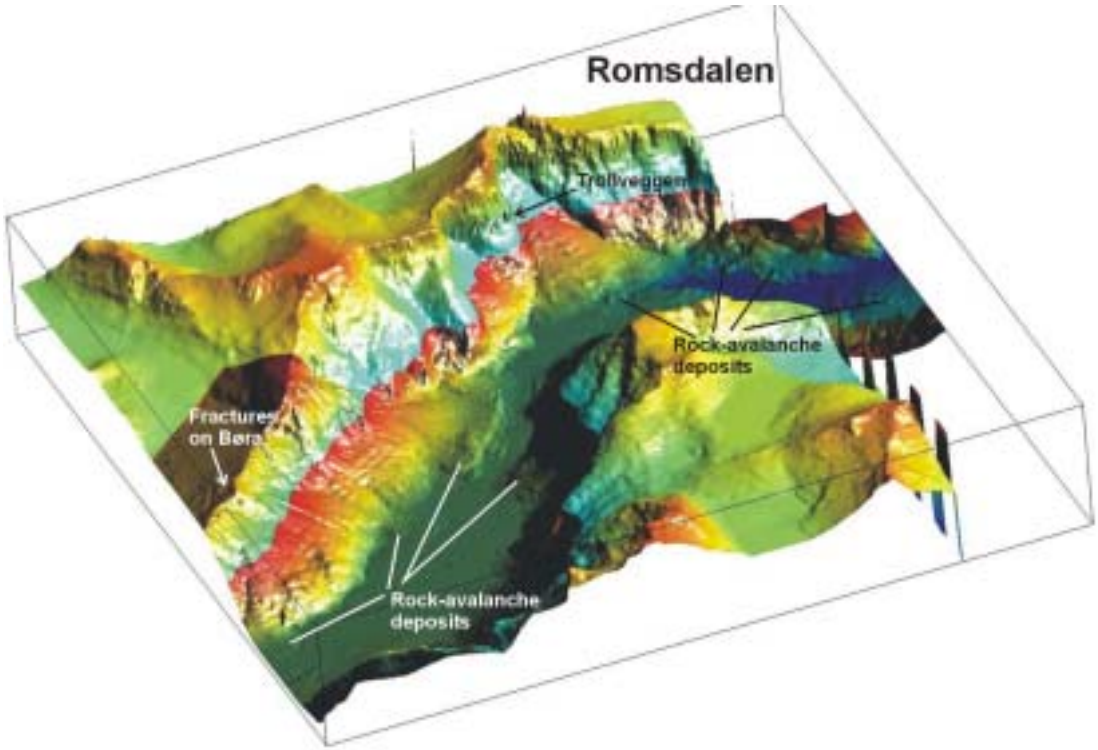

Figure 2. 3D image of Romsdalen based on topographic data in scales 1:50 000 (above 600 m asl) and 1:5 000 (up to 600 m asl). Note that large parts of the valley is affected by rock avalanches, shown by lobes and irregular surfaces. Details of the fractures on Børa (left-hand side of the model) are shown in Figs. 5-8.

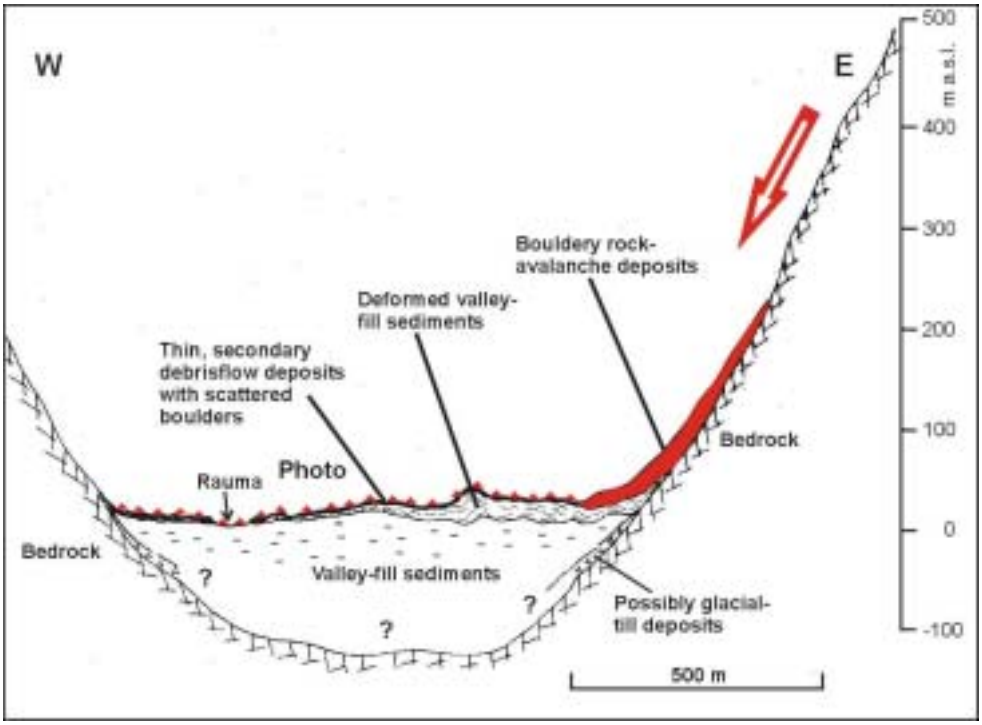

Figure 3. Schematic sketch from the Venje event in Romsdalen showing sediment distribution and effects of a large rock avalanche impacting valley-fill sediments.

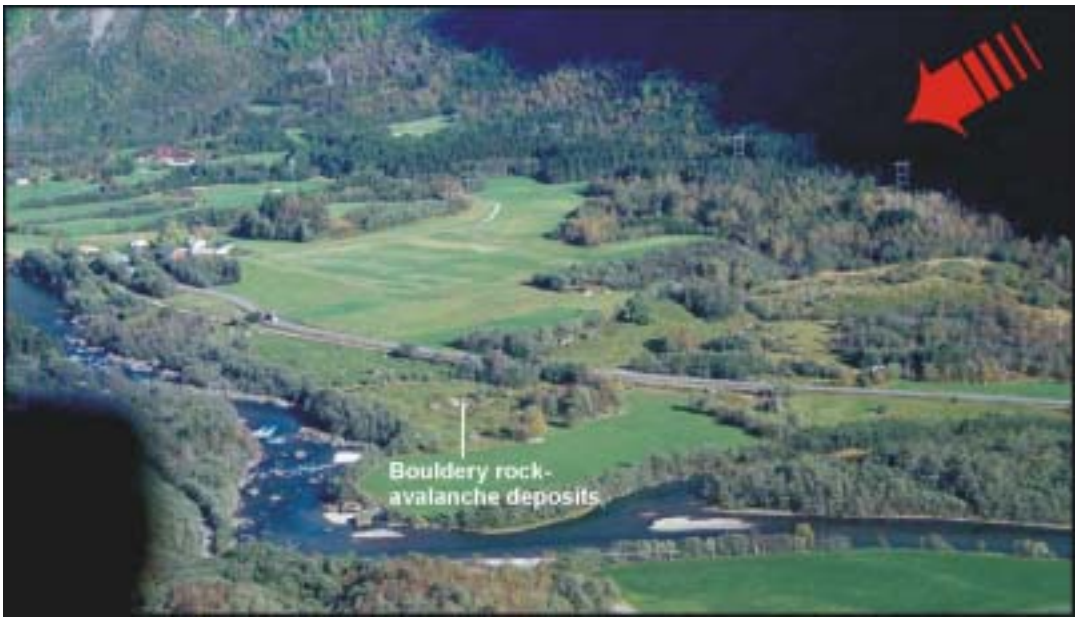

Figure 4. Overview of the Venje area, which is characterized by a bouldery and hummocky surface. The arrow indicates the direction of the avalanche, which was from the eastern mountain side. The distal part of the rock-avalanche deposits are covered by a thin sediment cover interpreted to be formed by secondary debrisflows (see approximate location in Fig. 3).

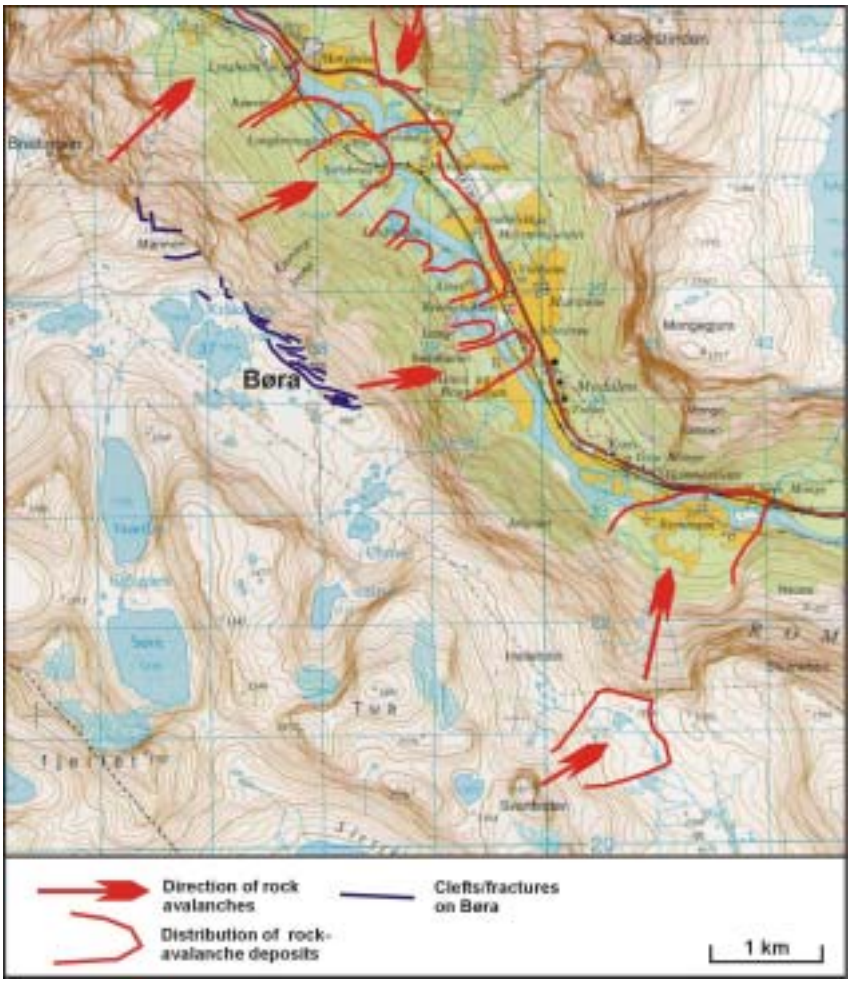

Figure 5. Topographic map from Romsdalen showing fractures on Børa, and the distribution of rock-avalanche deposits.

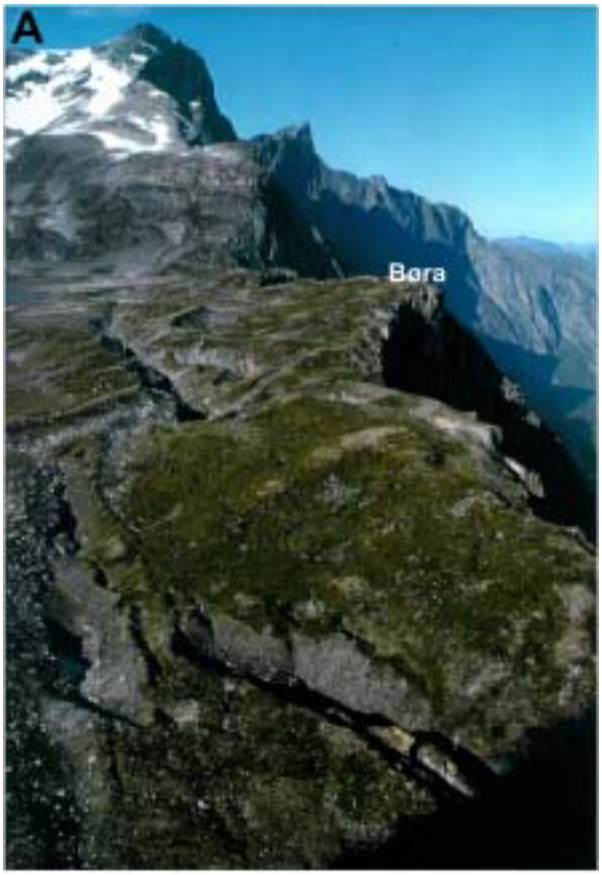

Figure 6. The unstable mountain plateau on Børa in Romsdalen seen from a helicopter. Note the deep and long fractures, cutting into glacial till and bedrock. View towards northwest.

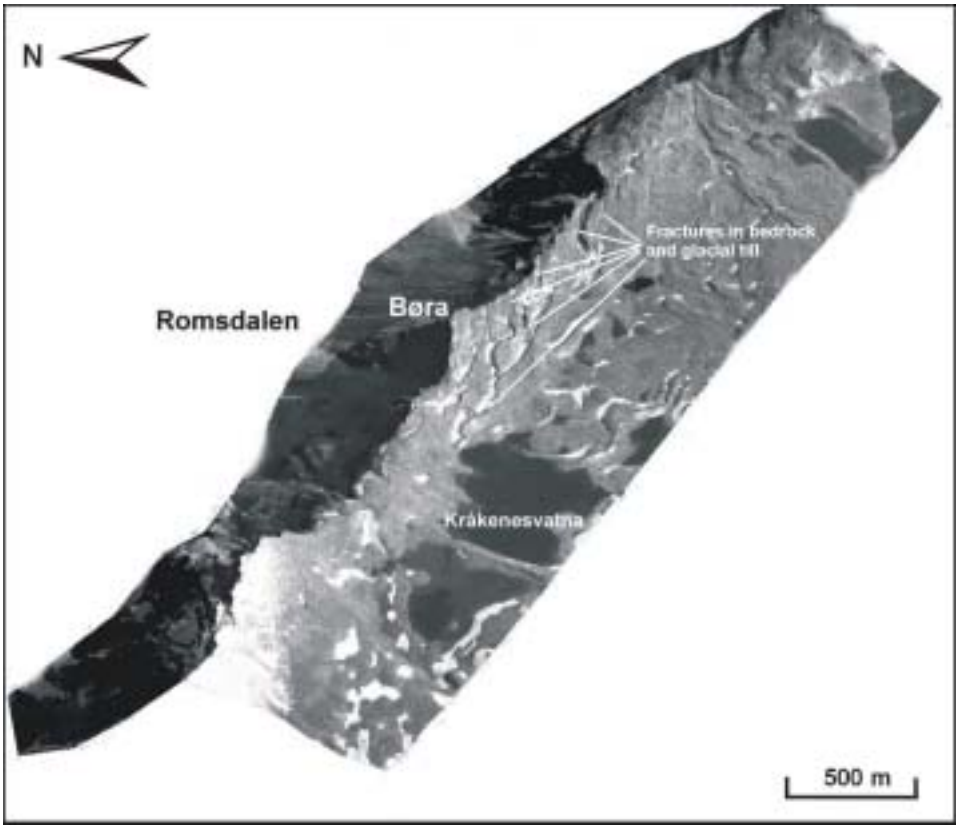

Figure 7. 3D model of the Børa area based on detailed topographic data and draped by orthophoto. View towards east.

Figure 8. The largest cleft in the Børa area. Note person for scale.

3.1.2 Tafjord – Geirangerfjorden - Sunnylvsfjorden

The Tafjord area has been investigated in great detail, in particular because the area experienced one of the most serious natural disasters in Norway. About 3 mill m^3 of rock and talus material dropped into the fjord in 1934, and the tsunami generated by the avalanche reached a maximum of 62 m above sea level; 40 persons were killed. The geological mapping reveals a high number of slide scars in the fjord slopes, and about 10 large rock-avalanche deposits are recorded in the fjord (Figs. 9-11).

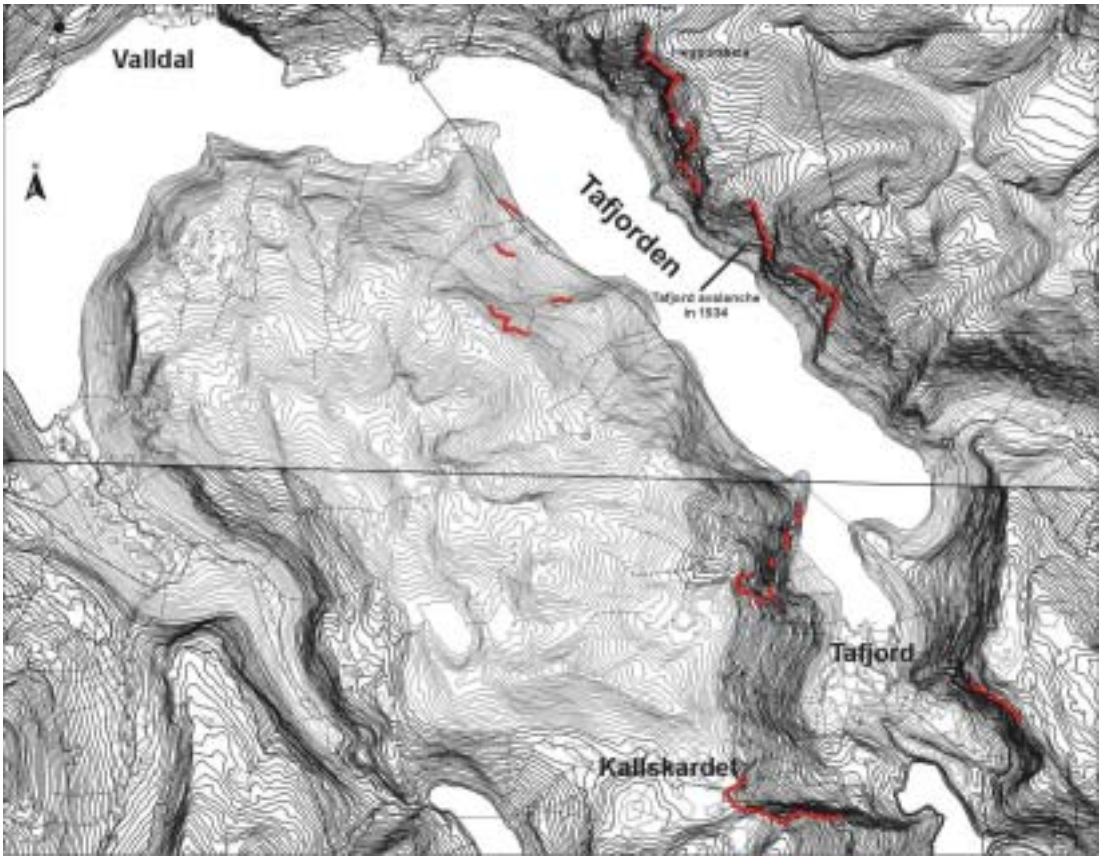

Figure 9. Topographic map of the Tafjorden area. The most prominent slide scars are shown.

The swath batymetri shows clearly the morphology of the individual deposits (Figs. 10, 12 and 13). The stratigraphy, established from seismic data and a sediment core, demonstrates that individual events are spread throughout the postglacial time, but with a higher frequency in the second half of the Holocene (Fig. 11). Some of the largest avalanches have a cone-shaped morphology with a bouldery surface, while others are smaller and can be seen on the fjord bottom as distinct concentric wavelike features around a core of rock debris (Figs. 12 and 13). Most of the avalanches have caused severe deformations of underlying sediments (see concentric ridges in Fig. 13). Similar extensive folding and faulting of soft sediments are also observed in outcrops and on georadar data associated with rock avalanches on land. An enormous rock avalanche, estimated to be more than 100 mill m^3, occurs in Tafjord. The slide scar is on Kallskardet (Fig. 9), and the avalanche debris can be tracked into the fjord with an outrun distance of more than 2 km along the fjord bottom. Below the 1934 slide scar at least tree individual rock-avalanche deposits are identified, with the 1934 event being the smallest (Figs. 10 and 11). In addition to the boulder cone, an outer splash zone interpreted to be formed by secondary massflows are well displayed (Figs. 12 and 13). Similar deposits have been found in excavations in distal parts of some rock avalanches on land (see Figs. 3 and 4 from Romsdalen).

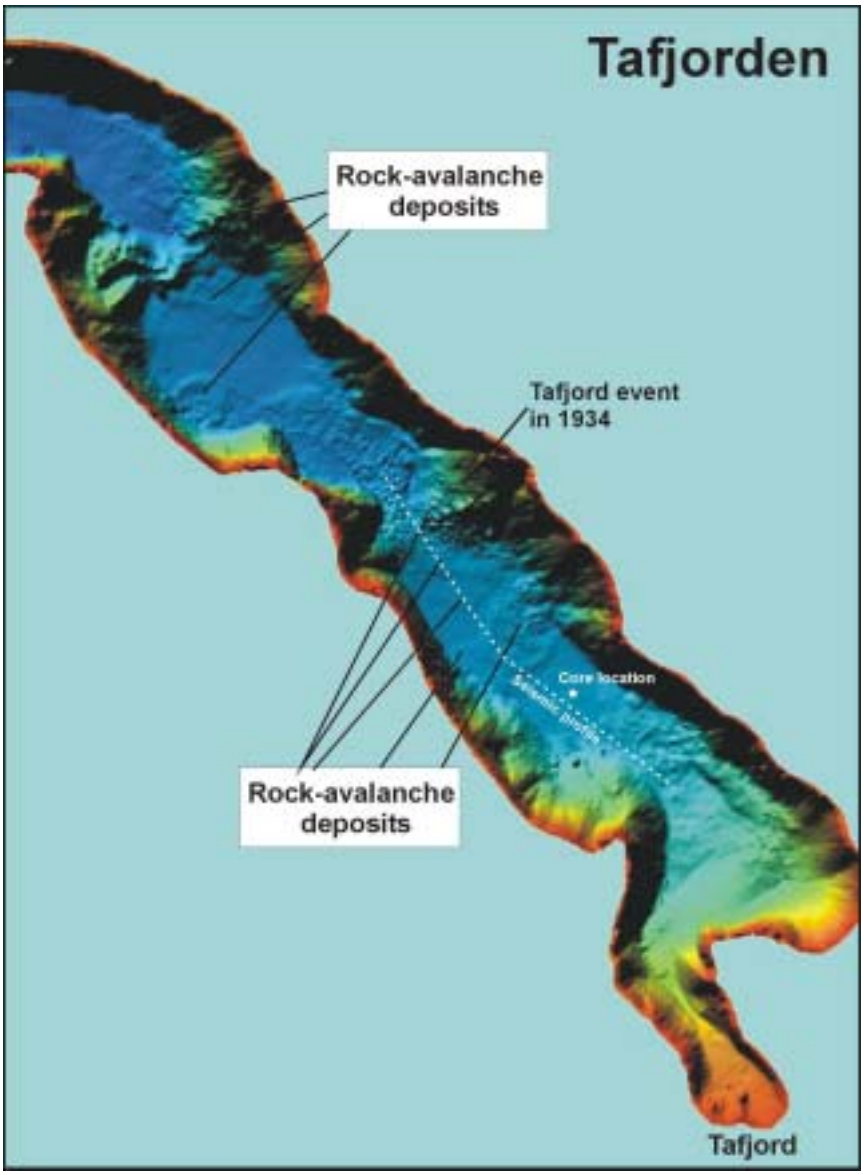

Figure 10. Shaded relief map from Tafjorden based on swath bathymetry.

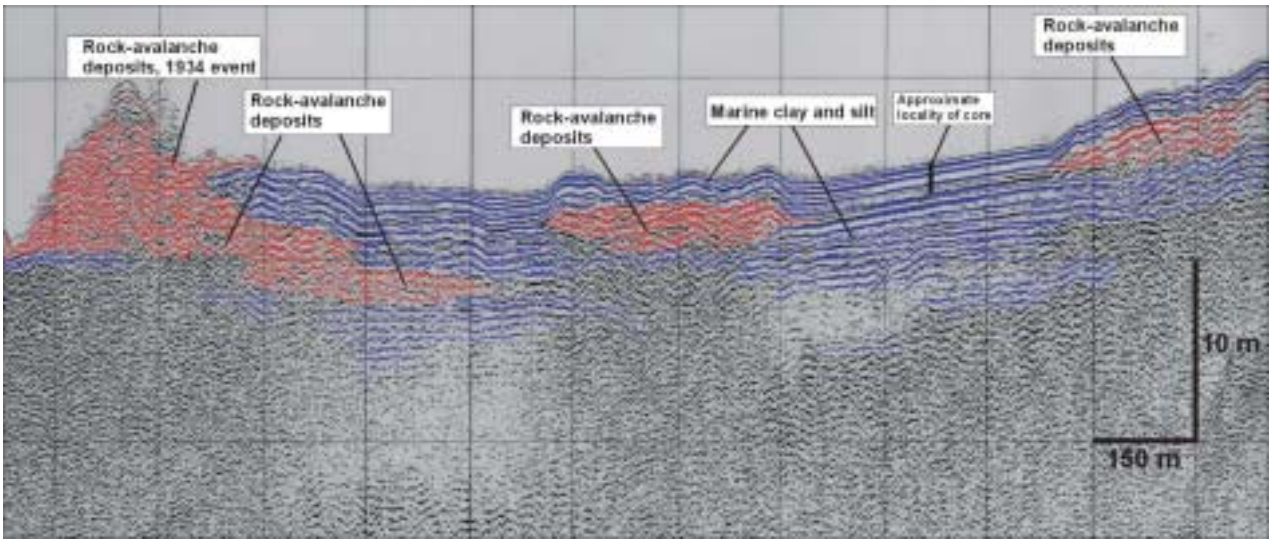

Figure 11. Seismic profile from Tafjorden showing the relationship between rock-avalanche deposits and finer-grained marine sediments. See location of seismic line in Fig. 10.

Two samples from a 1.2 m long core in Tafjorden have been dated (Fig. 14, see also Lepland et al., 2002). The location is shown in Fig. 10 and 11. The core shows several sand layers with erosive boundaries, where the lowermost probably is related to several rock avalanches (Fig. 11). The upper unit with an age of 658-564 cal. years BP (690±55 ^{14}C BP), lays below a relatively thick, normally graded turbidite or tsunami deposits, which may be related to the 1934 event (see also fig. 12). Altogether four events are recorded in the core, indicating that a series of rock avalanches have occurred after 3200-3000 calendar years before present.

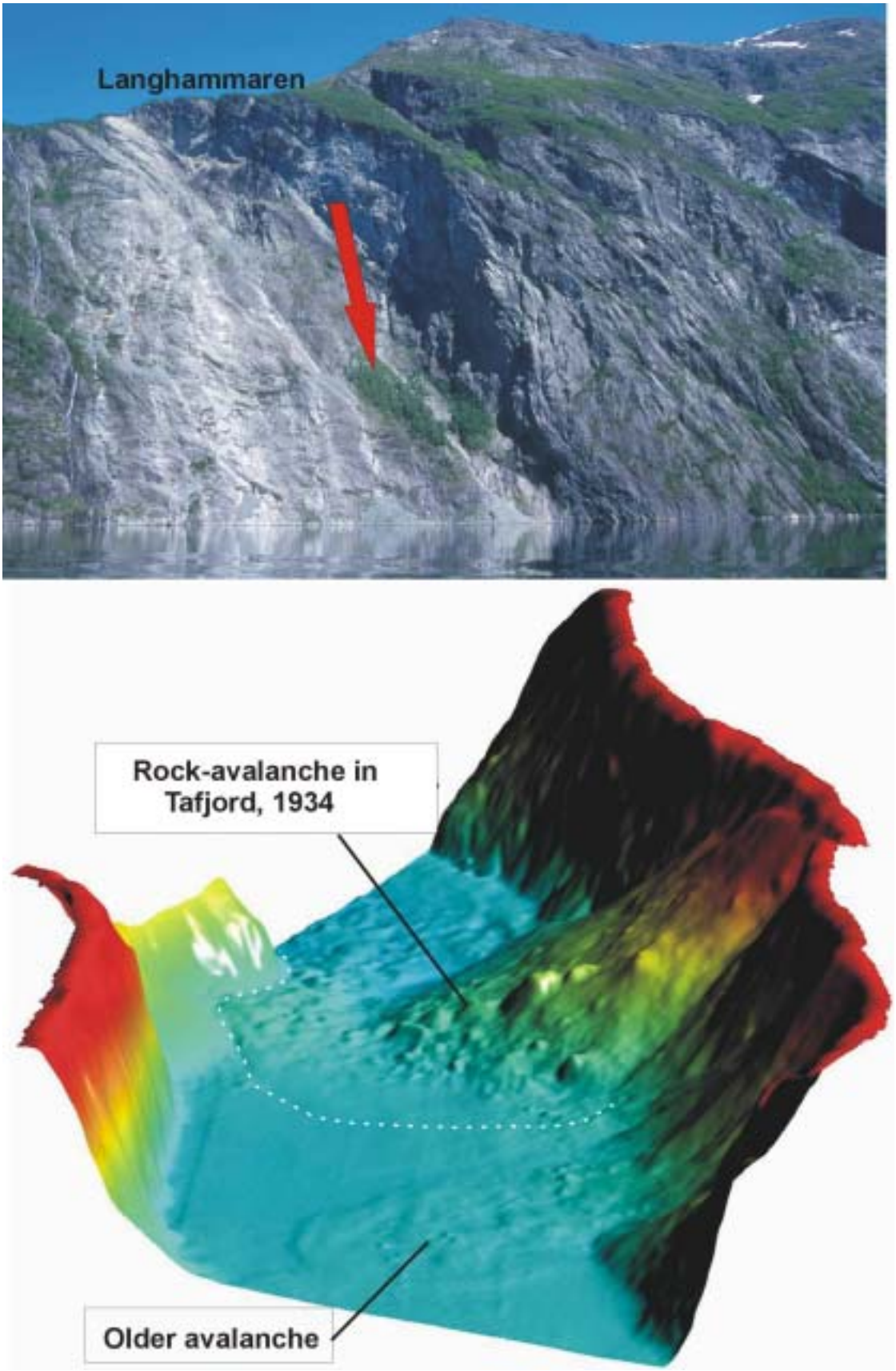

Figure 12. Langhammaren in Tafjord, with the slide scar of the 1934 event. The 3D image shows the rock-avalanche deposits in the fjord. The white stippled line delineates the outer limit of the avalanche deposits. Note also a smaller slide deposit in the foreground. View towards the north.

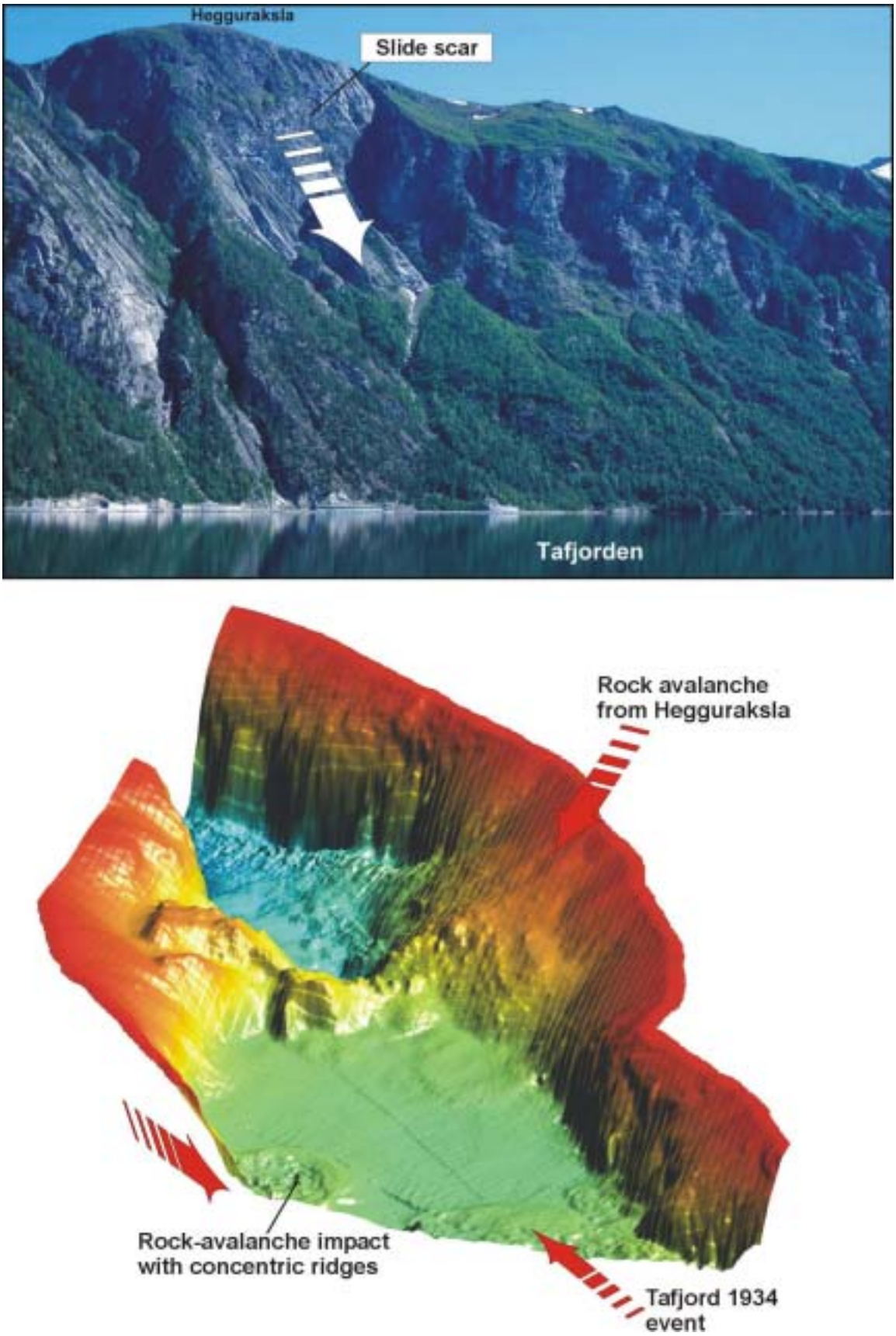

Figure 13. View of Hegguraksla with prominent slide scar. The 3D image shows the avalanche deposits in the fjord. Bouldery deposits from the Hegguraksla failure and the outer part of the Tafjord event in 1934 is clearly visible on the image.

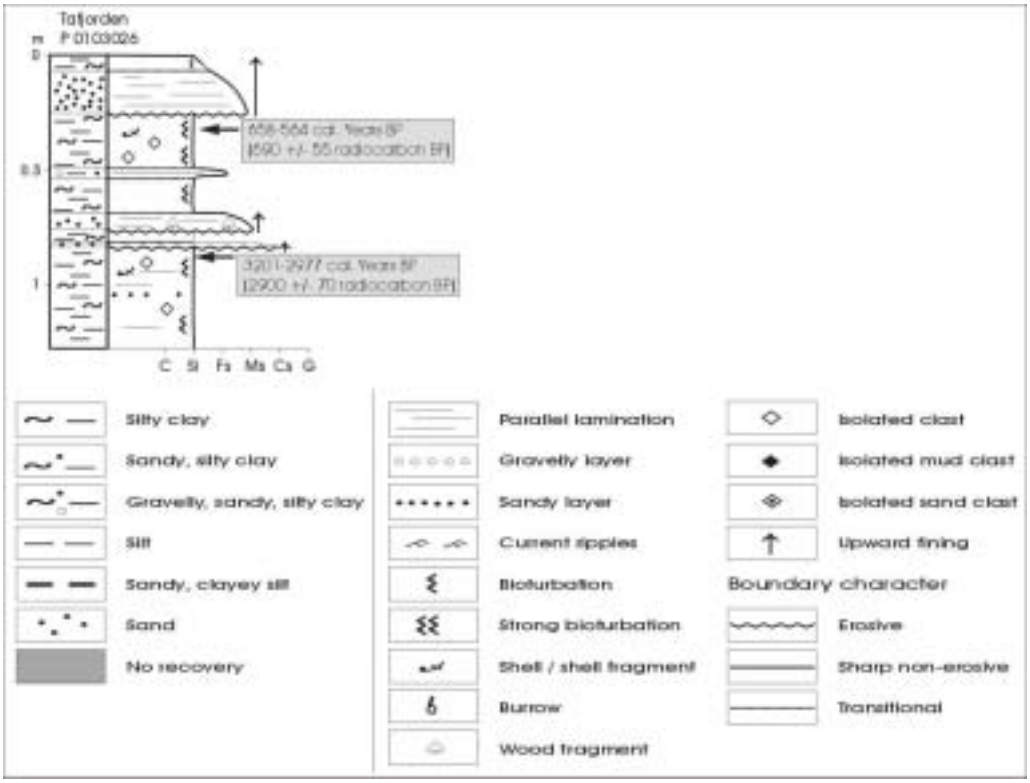

Figure 14. Core from Tafjorden. See locality in figure 10 and 11 (from Lepland *et al*., 2002).

Swath bathymetry and seismic data have also been gathered in Geirangerfjorden and Sunnylvsfjorden (see locality in Fig. 1). No cores exists, and the seismic stratigraphy is not yet well undrestood. The seismic and multibeam data demonstrate a high number of rock-avalanche events also in these fjords, and large areas of Geirangerfjorden are covered by bouldery rock-avalanche deposits (Fig. 15). They are, however, commonly smaller than in Tafjorden. The data from Sunnylvsfjorden also demonstrate several rock-avalanche deposits, many of them forming characteristic concentric ridges around the impact site on the fjord bottom (Fig. 16).

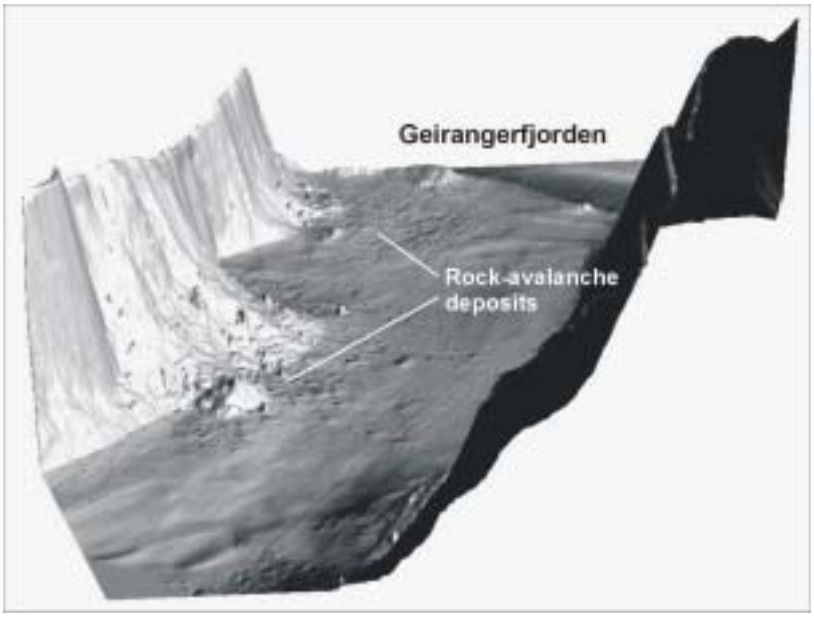

Figure 15. 3D image showing large bouldery rock-avalanche deposits in the outer part of Geirangerfjorden.

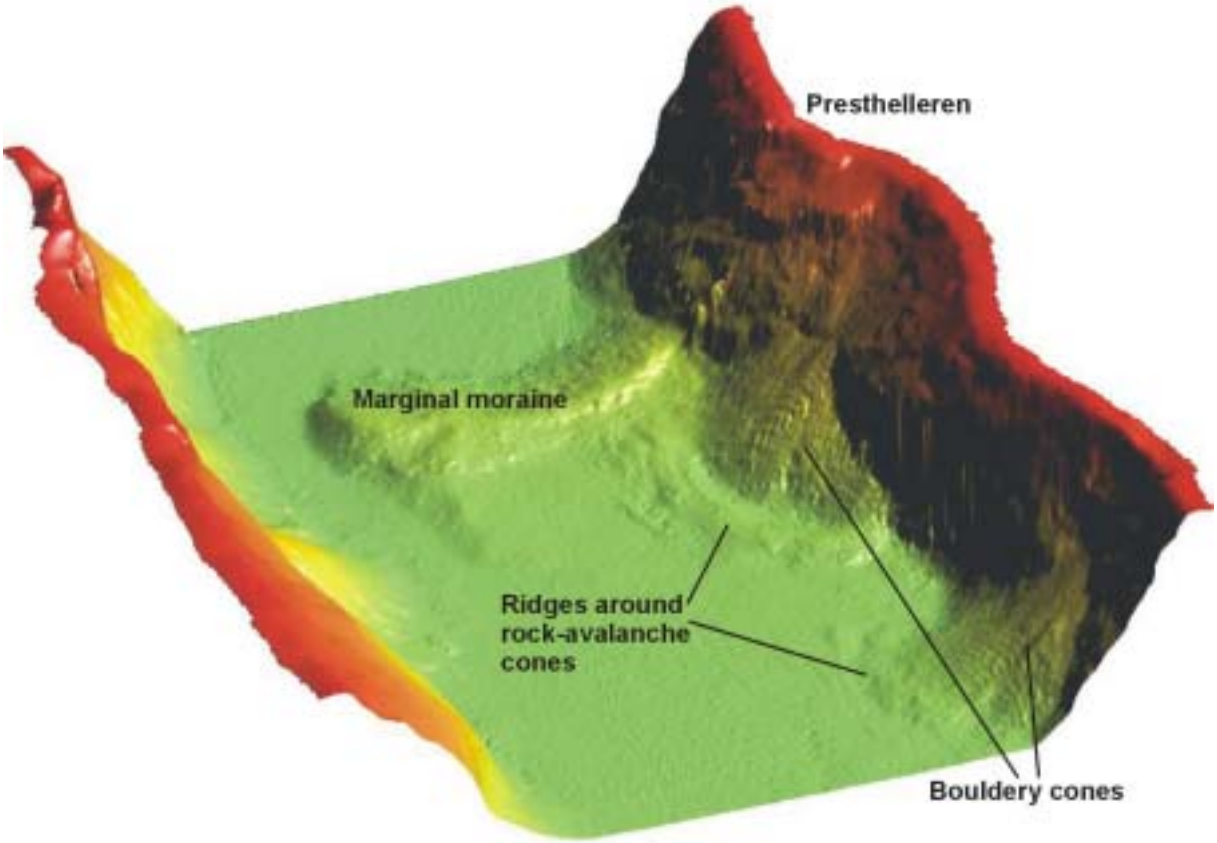

Figure 16. Rock-avalanche deposits and a marginal moraine in Sunnylvsfjorden. The failure from Presthelleren is described in historical documents. Note the well-defined ridges around the bouldery cones.

3.2 Coastal areas of Møre & Romsdal

3.2.1 Øtrefjellet

Øtrefjellet is situated on the peninsula northeast of Ålesund, see locality in figure 1. A bedrock ridge that is 2 km long, 50-150 m wide and 100 to 300 m high, is characterised by deformations in the form of fractures and clefts (Fig. 17, see also Anda *et al*., 2001). The clefts have two main orientations, one sub-parallel to the ridge (SSW-NNE) and one almost transverse to the ridge (E-W). Areas of the ridge are completely shattered (Fig. 18). The ridge is surrounded by a series of large rock-avalanche deposits (Fig. 17), demonstrating that large portions of the flanks of the Øtrefjellet ridge have collapsed. In detail, bedrock failures, demonstrated by well-defined slide scars, have developed into large rock avalanches with well-defined frontal lobes. One of these extends into the small lakes Vestrevatna on the eastern flank (Fig. 17). Age-wise, the features observed on Øtrefjellet are postglacial, since they are situated far below the upper limit of the maximum Weichselian ice sheet.

Parts of the mountain slopes on Øtrefjellet have a gentle gradient, which hints at other causes for slope failures than to gravity alone. If the observed bedrock fractures and large rock avalanches were triggered by one event (e.g. a large magnitude earthquake), it becomes important to try to date the event. With basis in this reasoning, and since the rock avalanche has moved into the lake on the eastern flank, we expected signals in the lacustrine sediments. Distinctive units would be a turbidite or a dust layer from the bedrock failure. Three stratigraphic cores were taken from the lake, in addition to a series of inspection cores. No

signs of turbidites or dust fall-out were found in the cores (Fig. 19). Fine-grained clay and silt are found at the base, interpreted to be deglaciation sediments. These sediments are capped by first gyttja and silt of 5 cm and then by a 10 cm thick diatomite. The Vedde ash bed is found in the middle of this unit. The diatomite unit is then capped by 130 cm thick gyttja, without minerogenic sediments. The Vedde ash layer demonstrates that the core samples the entire Holocene, Younger Dryas and probably back to the deglaciation some 14-15.000 calendar years before present. Since there are now signs of the rock-avalanche event, it is concluded that it is old, probably from the deglaciation stage. An alternative options is that the rock-avalanche itself did not reach the lake, but that the bouldery deposits have been further transported down to the lake shore as a rock-glacier. This could have happened during the Younger Dryas period when permafrost conditions prevailed in this region. Anyway, the missing geological evidence here points to the conclusion that the bedrock failures occurred prior to the end of the Younger Dryas period.

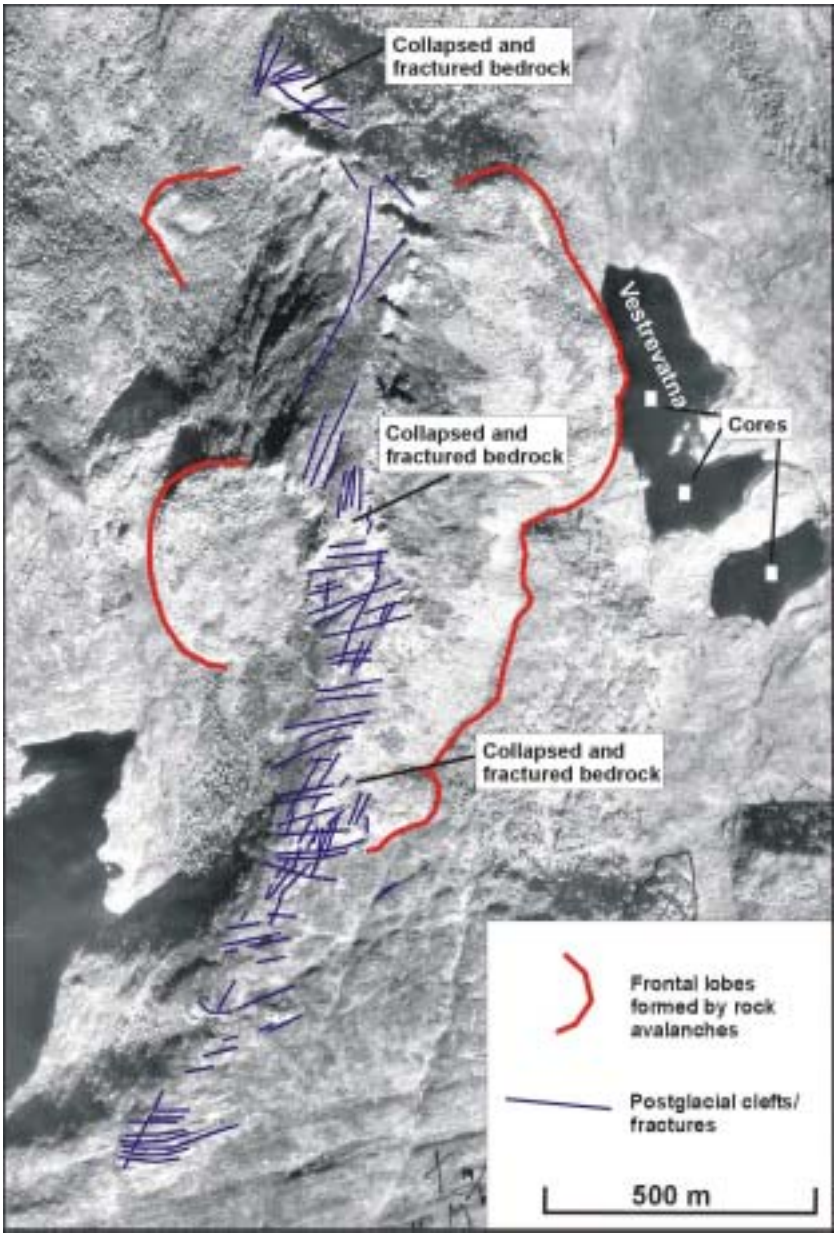

Figure 17. Aerial photo from Øtrefjellet showing distribution of rock avalanches and gravitational fractures. The northernmost core in Vestrevatna is shown in Fig. 19.

Figure 18. Bedrock outcrops on top of Øtrefjellet showing intense fracturing.

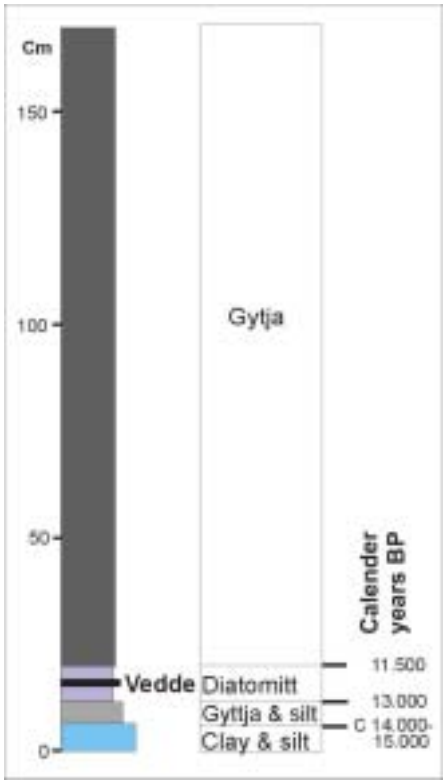

Figure 19. Core from Vestrevatna. The indicated dates are interpreted on the basis of time of deglaciation and the Vedde ash layer.

3.2.2 Oterøya

Several rock-avalanche deposits have been mapped on the northern part of Oterøya, approximately 15 km west of Molde (see locality in Fig. 1), and an unstable mountainside has been described along the southern slope of the island (Robinson *et al*., 1997; Blikra *et al*., 2001) (Figs. 20 & 21). Within an approximately 1 km wide and up to 700 m high slope, actually stretching from near-shore to the peak of Oppstadhornet, open crevasses and clefts reflecting block sliding, are found (Figs. 21-23).

The slide-block field is characterised by significant internal faulting/sliding marginal to larger collapse structures (Figs. 21-23). The field is bound by three key structures. In the SW, a NW-SE striking and steeply NE dipping fracture-zone, reactivating a Devonian (?) fault, is clearly visible. The fracture-zone forms a transfer structure that has seen highly down-oblique sliding. Above the field, the main, upward-bounding structure is clearly displayed as an escarpment. This structure is superimposed on the steeply SE-dipping foliation as well as a narrow zone of Devonian (?), carbonate-cemented fault breccia (Blikra et al., 2001). The upward bounding structure acted (or acts) as a master fault during collapse, as is easily seen by the large escarpment, steep and up to 20 m high. In the east, the termination of the collapse field is identified as a NNW-SSE striking and steeply SW dipping structure, which has acted as a transfer fault.
Internally, the slide-block field is segmented into large blocks by two sets of steep fractures; NW-SE and NE-SW striking. The latter set is sub-parallel to the master fault and the foliation in the rocks. The fault sets are different in that they show down-S transport on the NW-SE fractures and down SE transport on the NE-SW fractures, respectively. Many of the blocks in the field are rotated: Surface blocks rotate out from the slope, i.e. clockwise, in addition to the general down sliding, whereas the overall pattern of the collapse field is that of rotation toward the slope (anticlockwise) above a basal detachment.

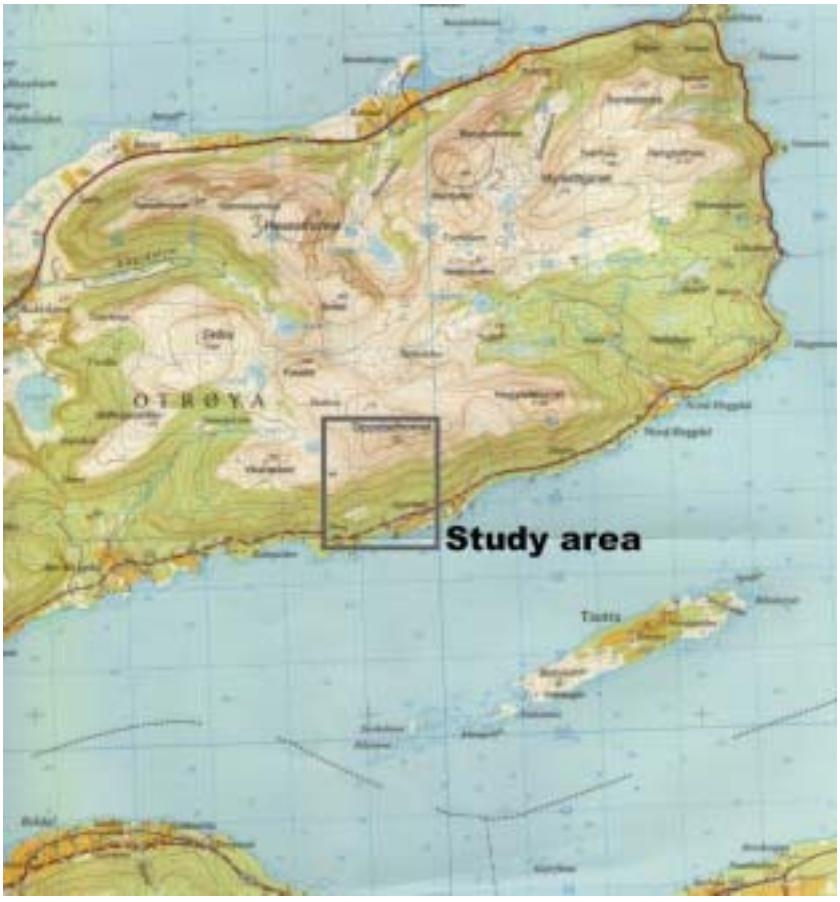

Figure 20. Topographic map (1220 II) locating the Oppstadhornet area.

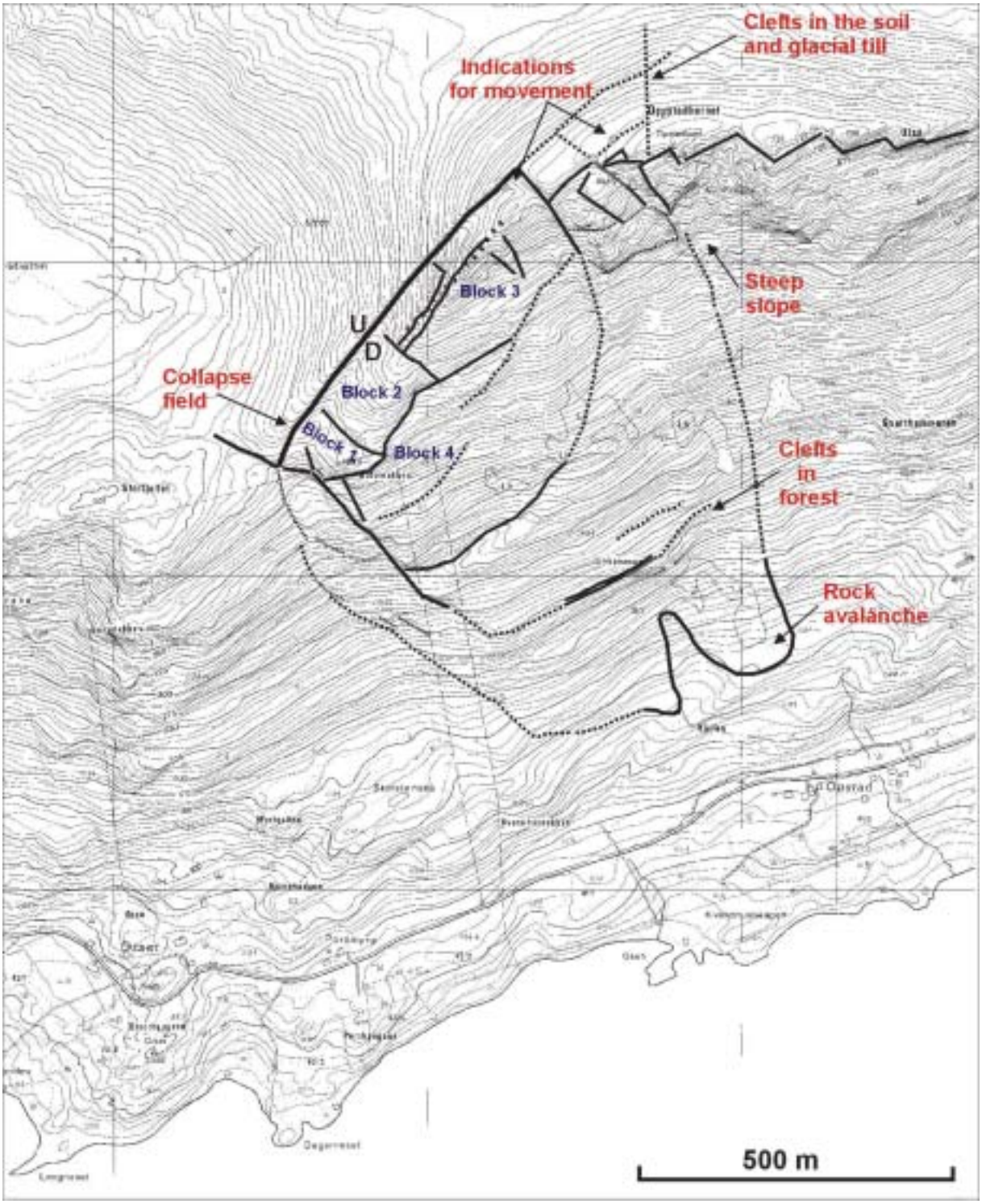

Figure 21. Detailed topographic map of the Oppstadhornet area, showing main structures of the collapse field (from Blikra *et al*., 2001). Heavy lines are faults, whereas dotted lines are inferred faults.

The steep slope to the east is characterised by fractures and fissures that reactivate the steeply SSE dipping foliation, and that generate moderately sized blocks. In addition, several mega-blocks are identified (Fig. 21). They are bound by similar fractures in the back, and some have slid 10-30 m down without being significantly internally shattered (Figs. 21-23). On the plateau around Oppstadhornet, there are several 1-2 m deep clefts in the soil and moraine

(Fig. 21). These relatively small structures indicate that fractures similar to those in and around the slide-block field are partly reactivated in this area as well.

In the lowland, near the foot of the mountain-side, at least two clefts have been observed. They are found approximately 10 m above small cliffs, and are characterised by blocks that have sunk 2 to 5 m, i.e. they appear as small grabens parallel to the cliff-face. They indicate that the entire slope down to sea level has experienced or experiences movements. One can speculate that a basal detachment for the overlying slide-block field actually emerges in this area, near sea level (Fig. 21). Some rock-avalanche deposits are found at the base of the collapsed slide block (Fig. 21).

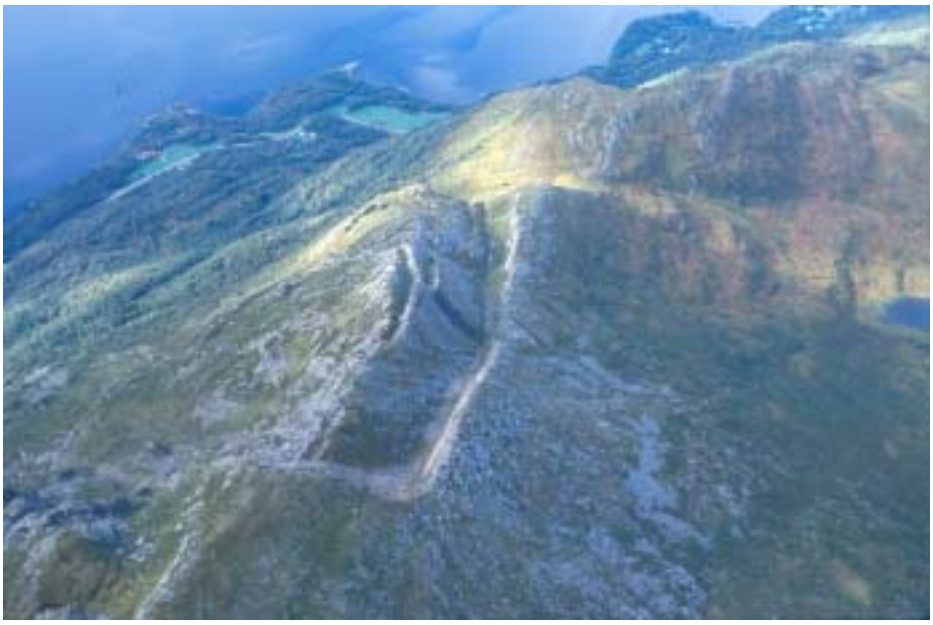

Figure 22. View from the north, showing the master fault in the back of the collapse field, and a major, wide-open cross-crevasse (from Blikra *et al*., 2001).

Figure 23. View from the southwest of the collapse field at Oppstadhornet. Note the bounding master fault and both strike-parallel and cross-fractures that subdivide the area into several blocks (from Blikra *et al*., 2001).

3.2.3 Sørdalen, Syvdsfjorden

A series of fractures occur on the mountain Storhornet (Fig. 24), south of Sunnylvsfjorden, (see locality in Fig. 1). A large slide block is sitting on the flank of the mountainside (Fig. 25A). Several rock avalanches have been initiated on this unstable mountain slope, and one has crossed the Sørdalen valley and climbed almost 50 m up on the opposite mountain slope (Figs. 24 and 25B). The entire southern part of the valley is characterized by bouldery and hummocky rock-avalanche deposits. Also the northern part down to the lake, shows distinct ridges with large blocks. Excavations show deformed valley-fill sediments, and only the upper part (less than 1 m) seem to be mass-flow deposits. The deformed sediments are interpreted to be formed due to rock-avalanche impact and secondary debrisflows. Small bouldery ridges still stands above the river plain at an altitude of about 12 m above sea level, without being reworked by fluvial processes. It is concluded that the sea-level stand was no higher than 10 m during deposition of the rock-avalanche deposits, demonstrating that the events are at least younger than the Younger Dryas.

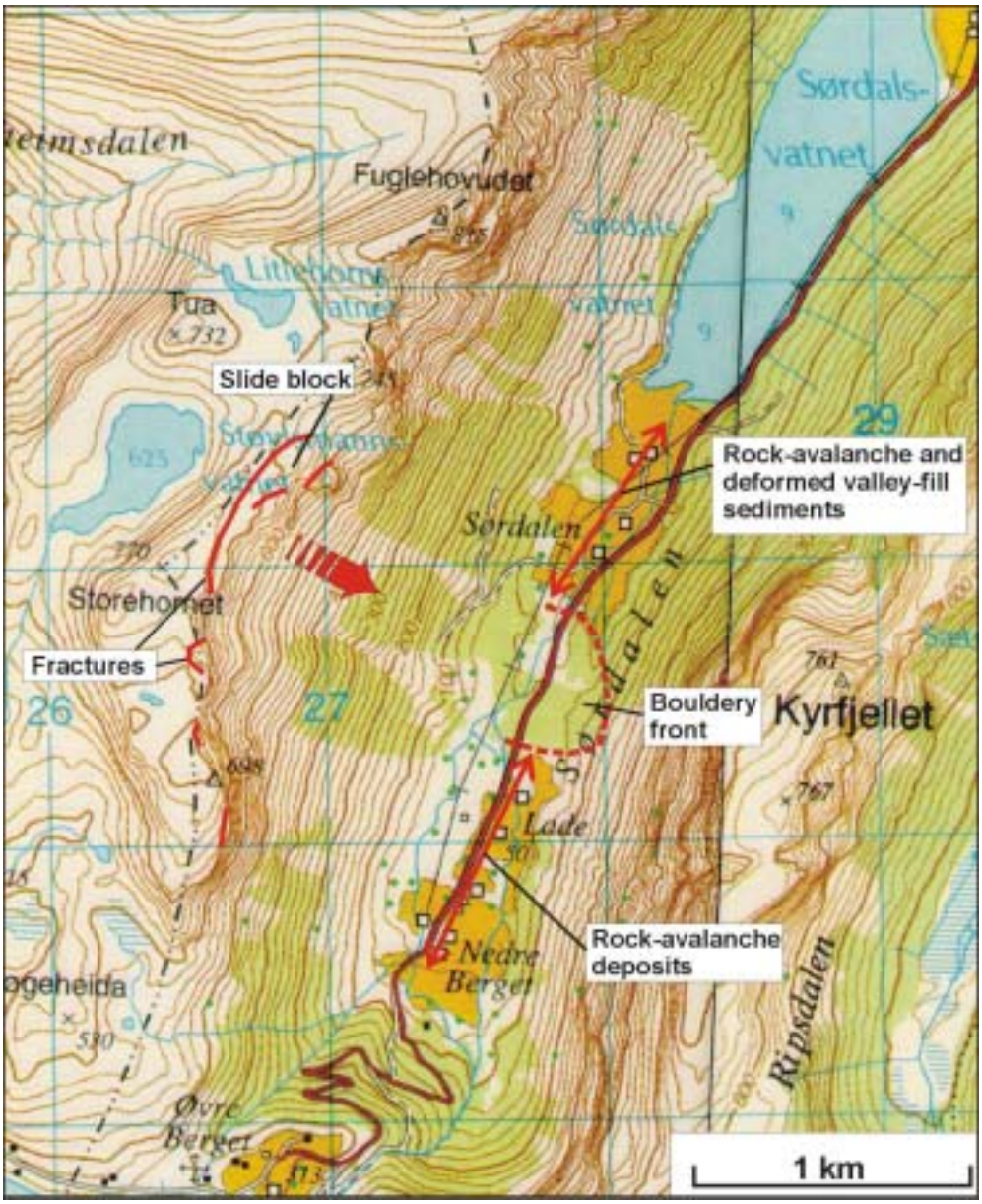

Figure 24. Topographic map showing slide blocks and fractures on Storehornet (Fig. 25A). Several rock avalanches are mapped in the valley Sørdalen (Fig. 25B).

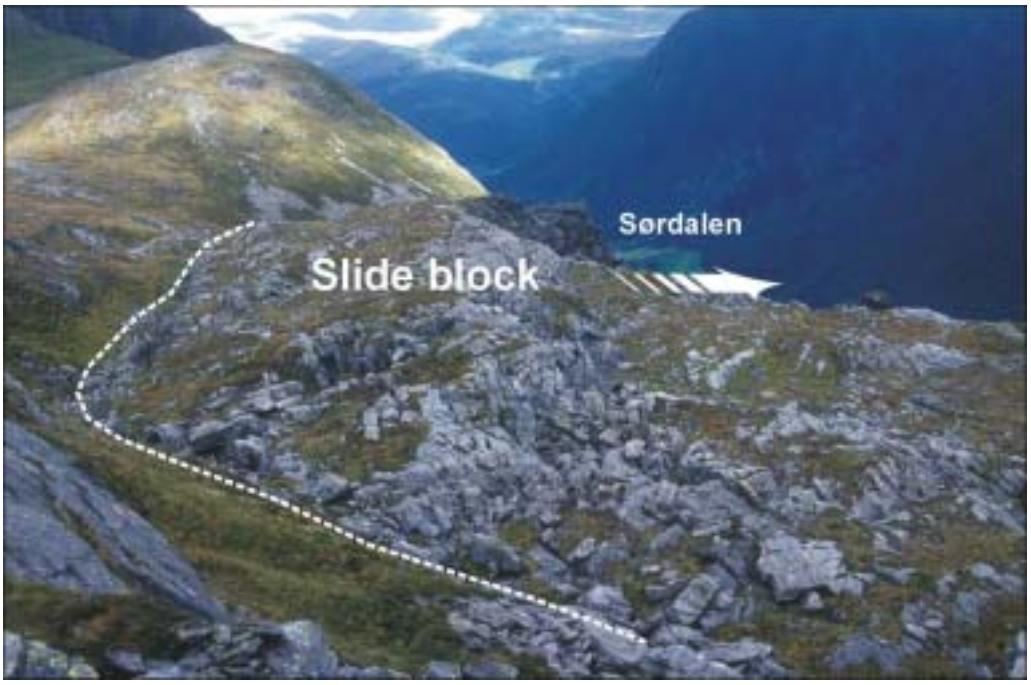

Figure 25A. The largest slide block north of Storehornet (see locality on map in figure 24). The bedrock is densely fractured within the mega-block.

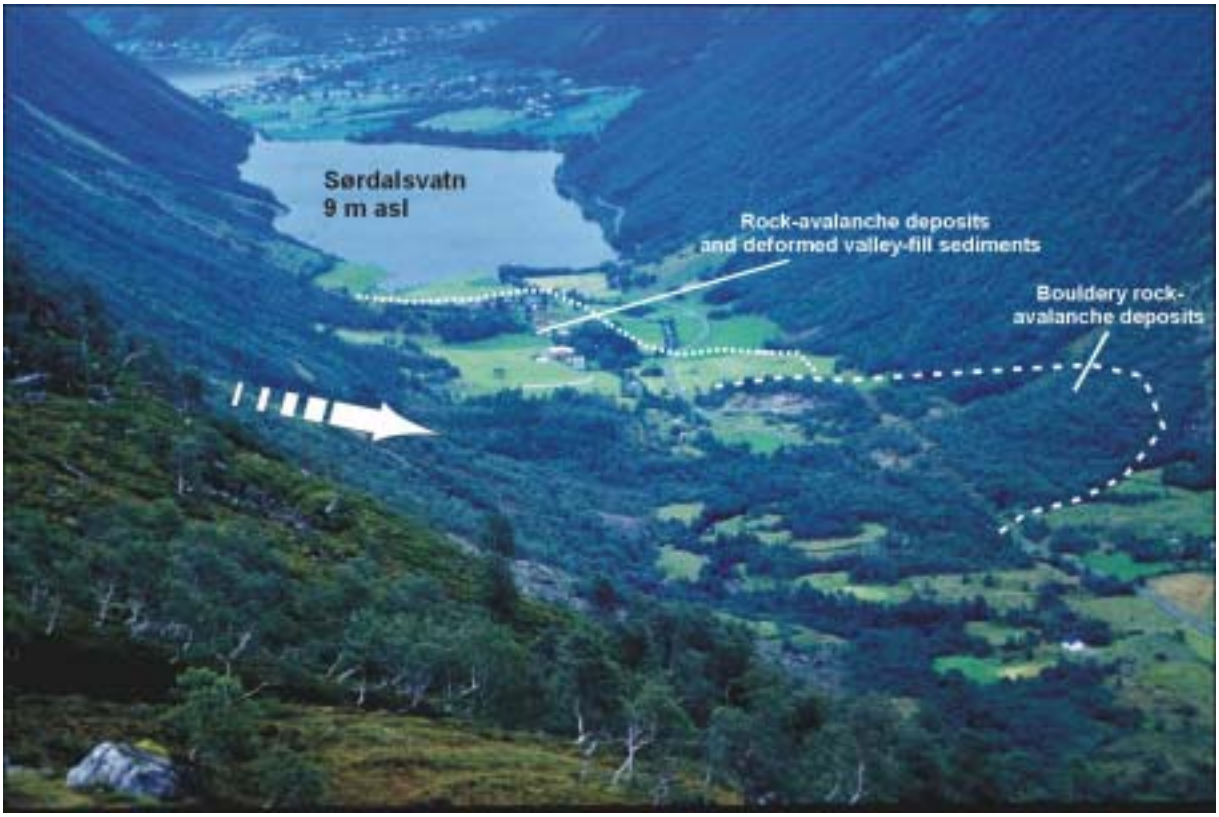

Figure 25B. View towards north along the Sørdalen valley to Syvdsfjorden. Note the distinct bouldery rock-avalanche lobe climbing up the opposite mountain side. The entire area down to the lake has been influenced by rock avalanches.

3.3 Sogn & Fjordane

3.3.1 Aurland

A range of instability features have been mapped in the phyllite areas of the Aurland-Flåm region (Fig. 26), Sogn & Fjordane (Blikra *et al*., 2000A, 2002). Geological mapping demonstrates that a series of rock avalanches, creep features and gravitational bedrock fractures occur in a zone that is 11 km long (Fig. 27).

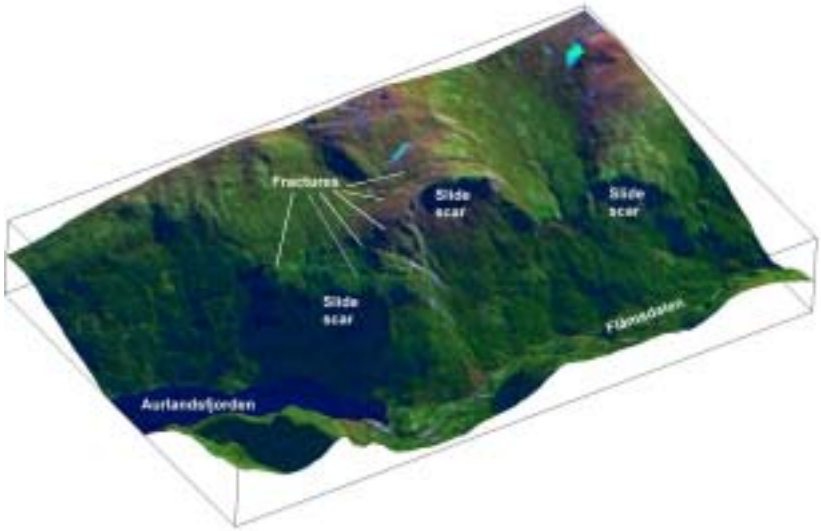

Figure 26. Gravitational fractures and slide scars in Flåmsdalen and Aurlandsfjorden. 3D model based on satellite and topographic data. View towards southeast.

Gravitational faults and fractures

Instability features are bound to the east by a series of normal faults, some showing local sink holes on the plateau (Figs. 27-29). One of the fractures displays an en-echelon over-step pattern (Figs. 29 & 30). Along its continuation, it is seen as a normal fault with a 1-2 m high scarp. This feature can be followed for about 4 km (Figs. 28 & 29). In the northern part of the area, slide structures in bedrock and glacial till are associated with the fault zone. The northern part of the mountain Ramnanosi is characterised by several N to NNW trending faults and joints. They are cut by a series of transverse fractures, which are parallel to the steep mountain side above Aurlandsfjorden (Figs. 28 & 31).

It is concluded that the entire mountain area west of the eastern boundary faults has moved several metres down to the W (see Blikra *et al*., 2002). If the thickness of the slide block is 300-500 metres, the total volume is between 900-1500 mill. m^3. Rock avalanches found along Flåmsdalen and in Aurlandsdalen are not included in this estimate. It cannot be excluded that the faults are of a tectonic origin, but gravity most likely was the controlling factor.

Slide features on land

A series of slide scars are prominent along the entire eastern mountainside of Flåmsdalen and Aurlandsfjorden (Figs. 26-28 and 32). In Flåmsdalen, large portions of the eastern slope are characterised by 100-700 m wide bouldery tongues (Fig. 33). The tongues are deposited in an imbricated fashion, with characteristic steep fronts and internal flatter areas. They are interpreted to be formed by creep processes originating from rock-avalanche deposits (Blikra *et al*., 2002). Similar features also occur along Aurlandsfjorden. Slide features in bedrock and glacial tills on relatively moderate slope gradients (16-24º), have also been observed in the mountain areas (Blikra *et al*., 2002). It is not common to find gravitational failures on such moderate slope gradients.

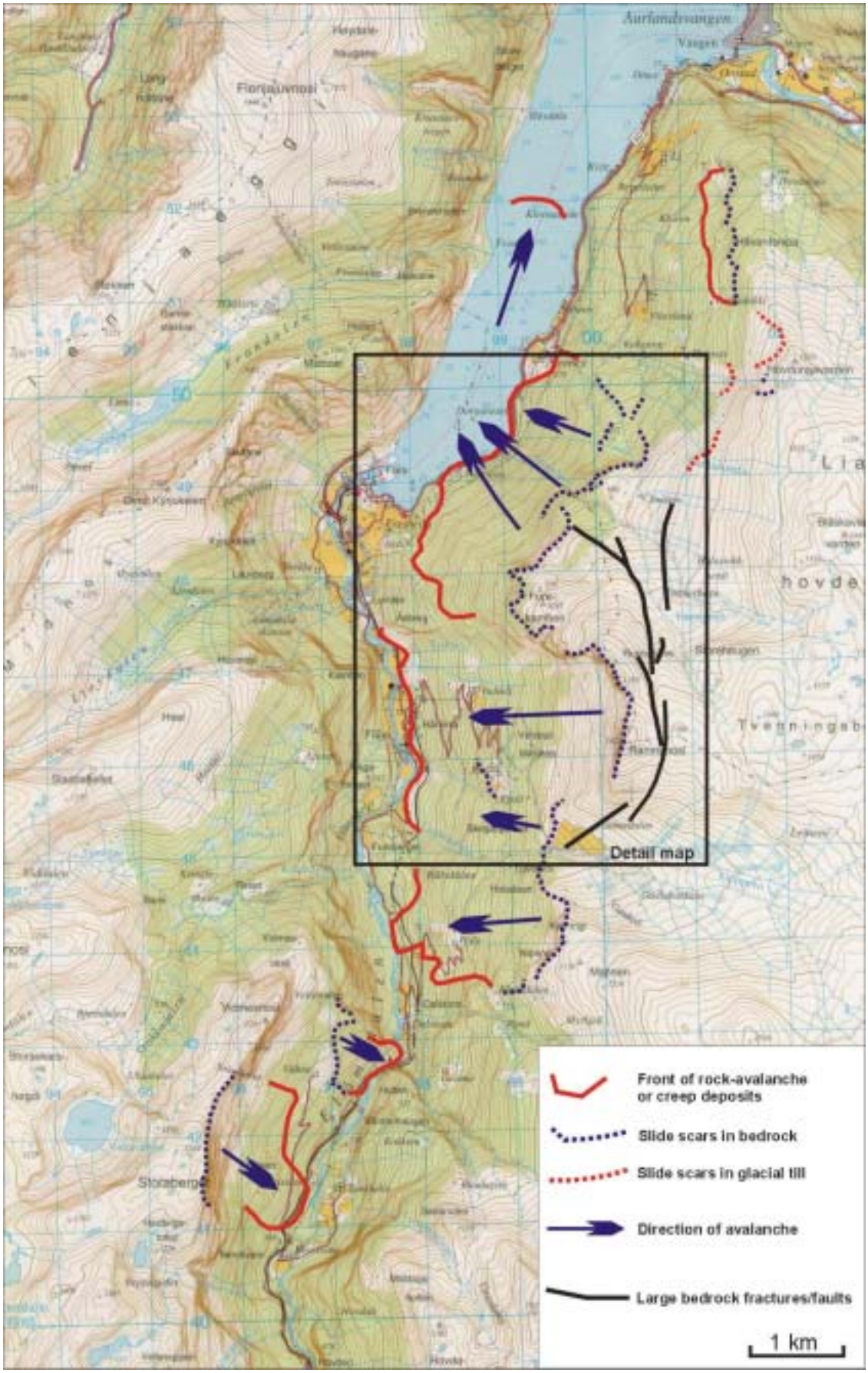

Figure 27. The studied area in Flåmsdalen and Aurland (Blikra *et al*., 2002). Major fractures and the main distribution of rock-avalanche and creep deposits are shown. Detail map is shown in Fig. 28.

Slides in Aurlandsfjorden

The morphology in the fjord shows large ridges, basins and hummocky deposits at the seabed (Fig. 34). The large ridges in the western part of the fjord are peculiar. They do not seem to be formed by rock avalanches from the eastern mountainside, where many large slide scars are prominent (see Figs. 28, 31 & 32). However, the morphology of the ridges and basins does not point to slides from the western mountain slope. The most viable interpretation is that the large ridges are bedrock features. The morphology on the fjord bottom shows one or more avalanche deposits in the eastern sector of the fjord, climbing partly up the bedrock ridges (Fig. 34). Their source area is on the eastern mountain slope.

A dense grid of seismic profiles was aquired in order to map stratigraphy and slide deposits (Blikra *et al*., 2002). The seismic data demonstrate that a large part of the inner fjord basin is filled by slide deposits. Fine-grained sediments are deposited in depressions in the slide surface (Fig. 34 & 35B), and only 2-4 m of younger sediments cover the avalanche deposits. An age of 2840-2720 calibrated years before present at 1,5 m depth in a core from Aurlandsfjorden (Figs. 35B & 36) indicates that the slide below is approximate 3000 years old. Much thicker sediment units are found in the basin between the two bedrock ridges (> 12 m; Fig. 35C). This indicates large differences in the age of the sediments in the bedrock basin compared to those capping the slide deposits. Fine-grained marine sediments are found below slide deposits further out in the fjord (Fig. 35A), and the sediment thickness above the slide deposits is here 5-8 m. Normally, the sediment thickness should decrease away from the delta area in Flåm, which is the main sediment input to the system. The sediment thickness above slide deposits is 2-4 m at a distance of less than 2 km from the delta, and more than 5 m at a distance of more than 4 km from the delta (Fig. 34). This indicates that there are several avalanche events in the fjord. The slides further out in the fjord is probably the oldest.

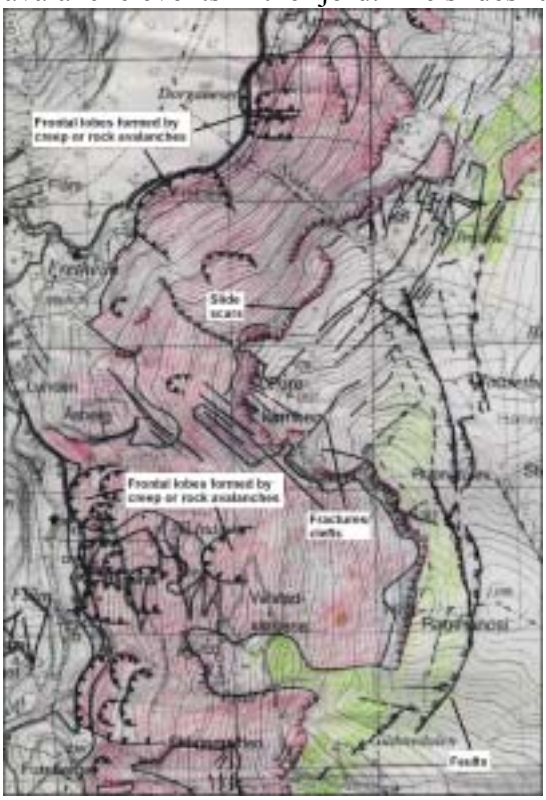

Figure 28. Geological field map from the lower part of Flåmsdalen and southern part of Aurlandsfjorden, see locality on Fig. 27 (modified from Blikra *et al*., 2002). Red colour shows areas covered by rock-avalanche or creep deposits, green colour is areas mantled by glacial till.

Age of fractures and rock avalanches

If the sedimentation rate shown in the core (Fig. 36) is representative for the Holocene period, the entire thickness of the postglacial Holocene sediments is between 4 and 5 metres. The sediment thickness capping the oldest slide in the outer part of the fjord (Figs. 34 & 35A) is consistent with that the largest and oldest slide occurred shortly after the deglaciation. The large bedrock failures and formation of widespread gravitational faults and rock avalanches in Flåmsdalen and along Aurlandsfjorden may have been formed during this event.

There is at least one younger rock-avalanche deposit in the fjord, derived from the phyllitic bedrock in the eastern mountain slope. Analysis of the sediment distribution and a radiocarbon age from a core indicate that the youngest rock avalanche in the fjord occurred some 3000 calibrated years before present

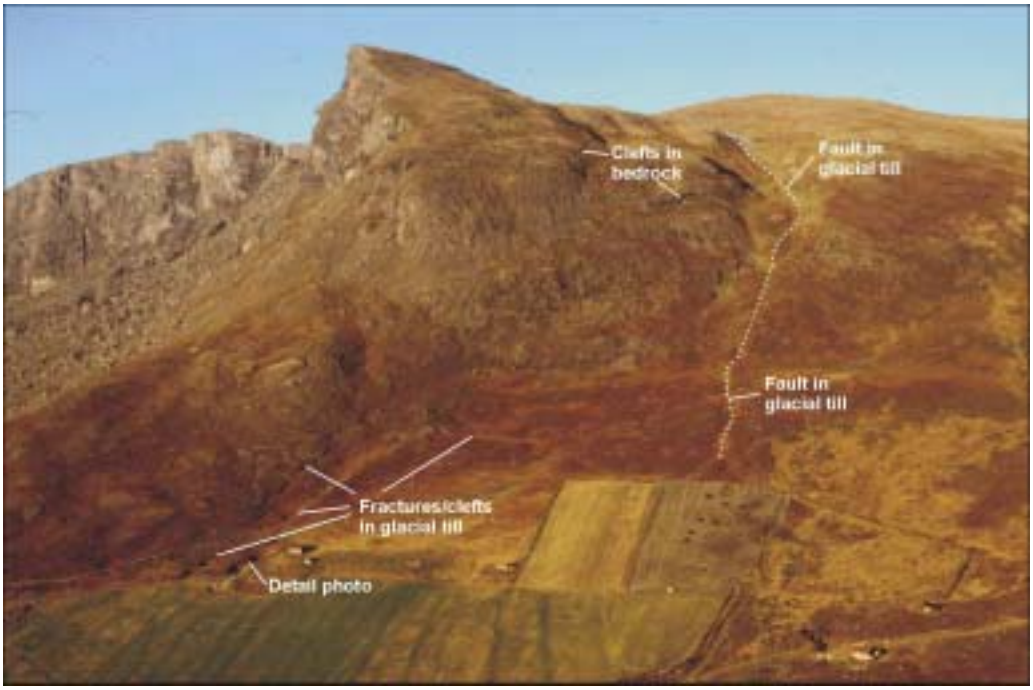

Figure 29. Gravitational faults and fractures in the area from Gudmedalen towards the mountain Ramnanosi (see map in Fig. 27; Fig. 28 for location). The photograph displays an approximate 700 m wide area in the lower part. Detail photo is shown in Fig. 30.

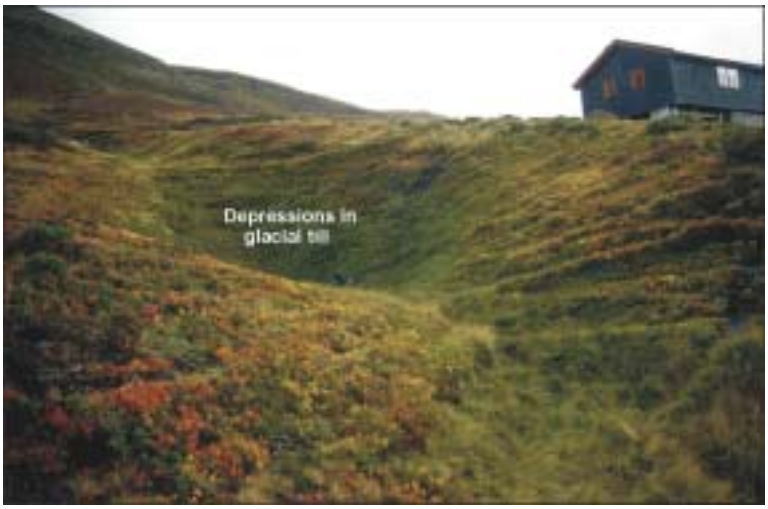

Figure 30. Depressions along well-defined clefts cutting thick glacial-till deposits in Gudmedalen (see locality in Fig. 29).

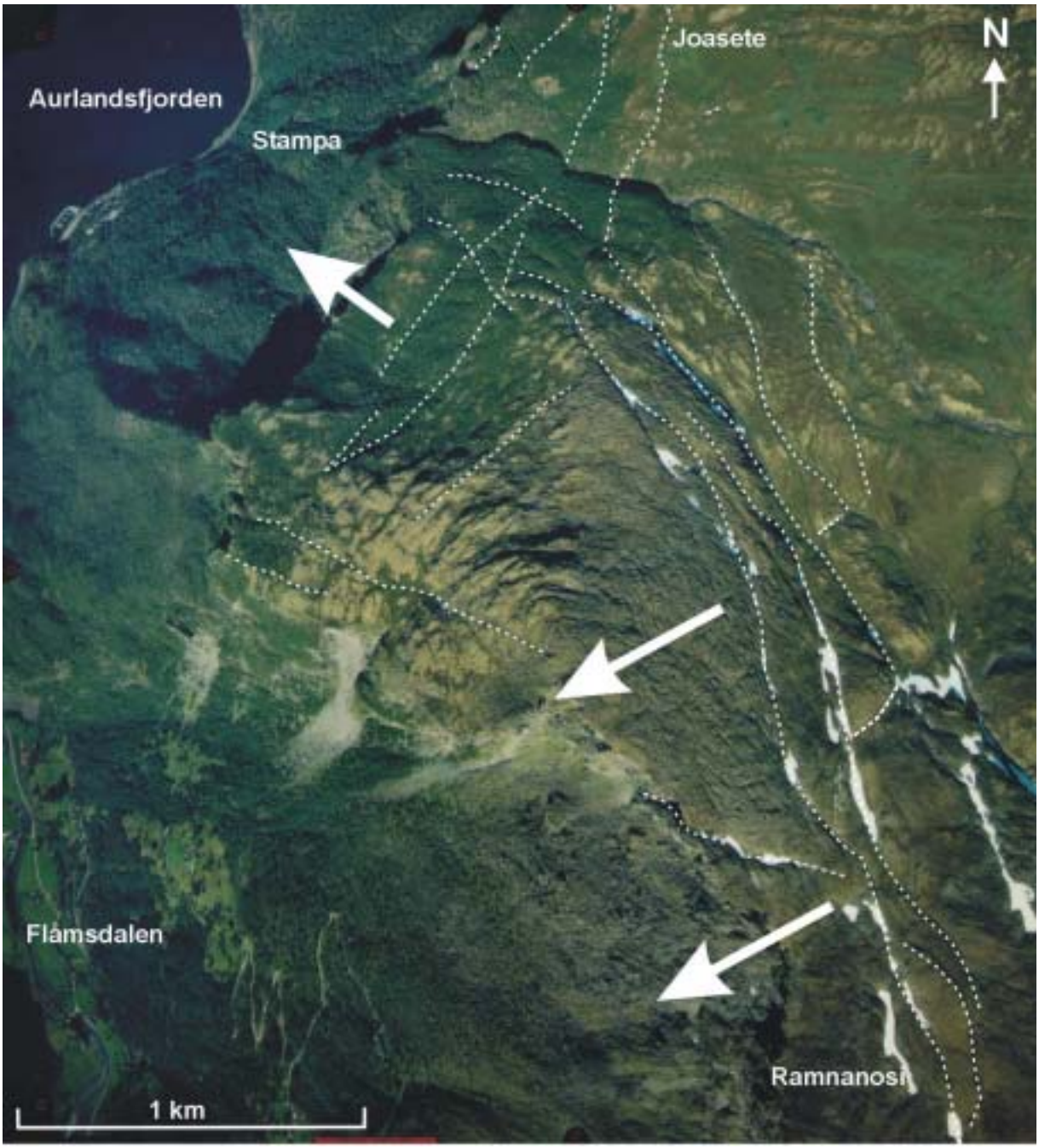

Figure 31. Aerial photograph from the area Ramnanosi – Joasete showing the main faults and fracture zones (see Fig. 27 for locality names). The overall pattern is consistent with that the entire area west of the fractures/faults has been downfaulted by several metres.

Figure 32. Slide scar between Flåm and Aurland. The scar is approximately 1 km wide. The rock-avalanche deposits are found in Aurlandsfjorden.

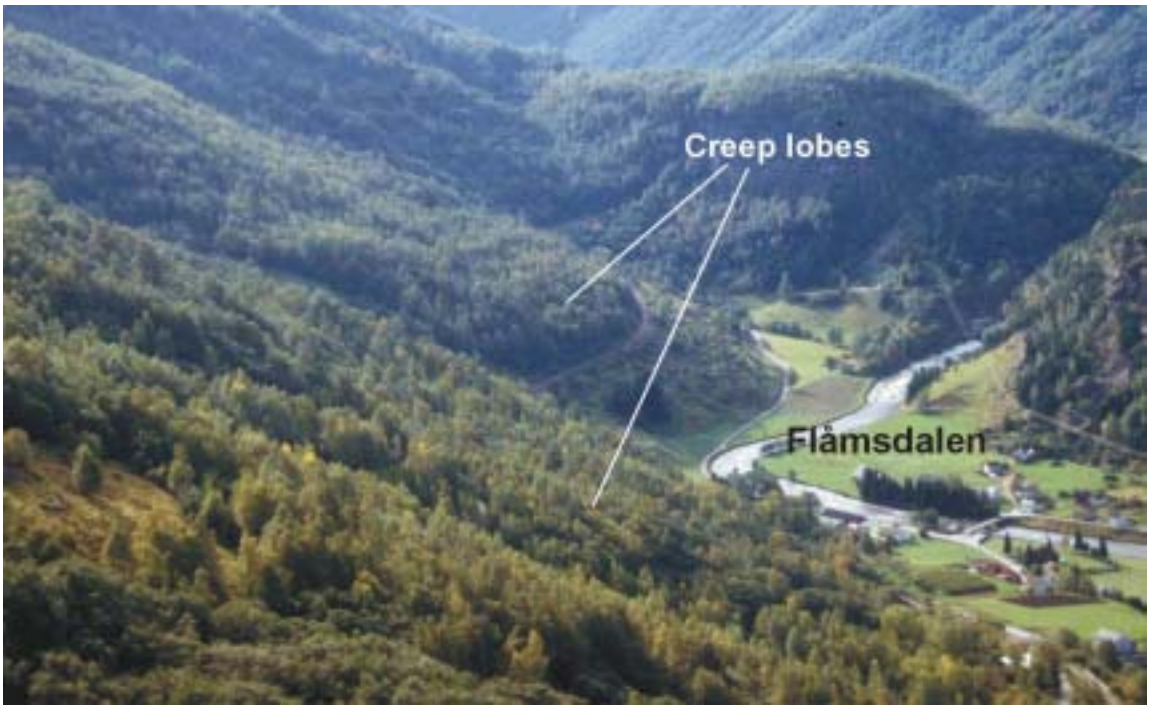

Figure 33. Well-defined lobes or tongues extending down to the river plain in Flåmsdalen. They are interpreted to be formed by creep processes, although originally deposited as rock-avalanches due to bedrock failures.

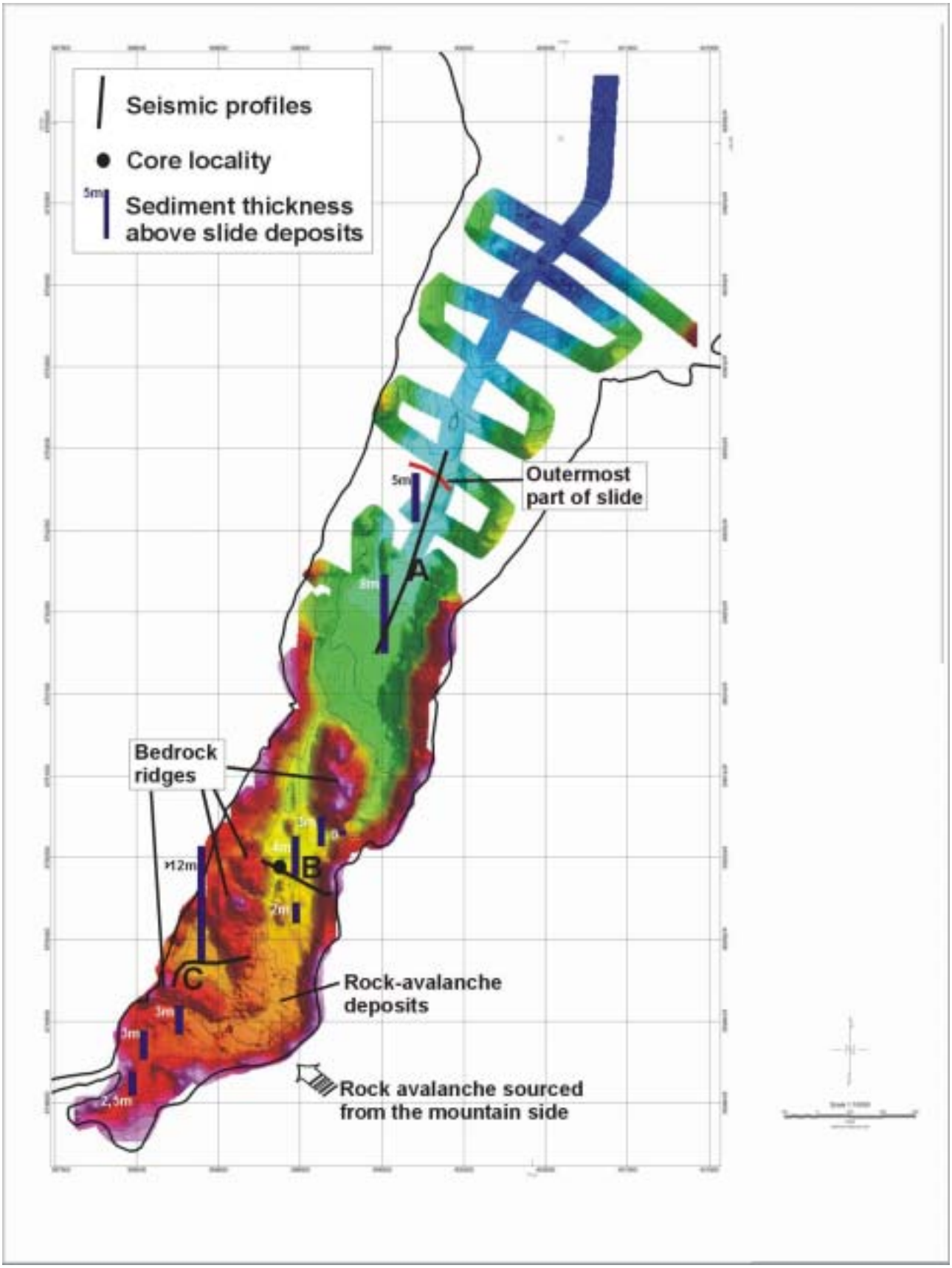

Figure 34. Bathymetric data from Aurlandsfjorden showing the main geomorphic features and sediment thicknesses above slide deposits (modified from Blikra *et al*., 2002). Three selected seismic lines are shown in Figs. 35A-C.

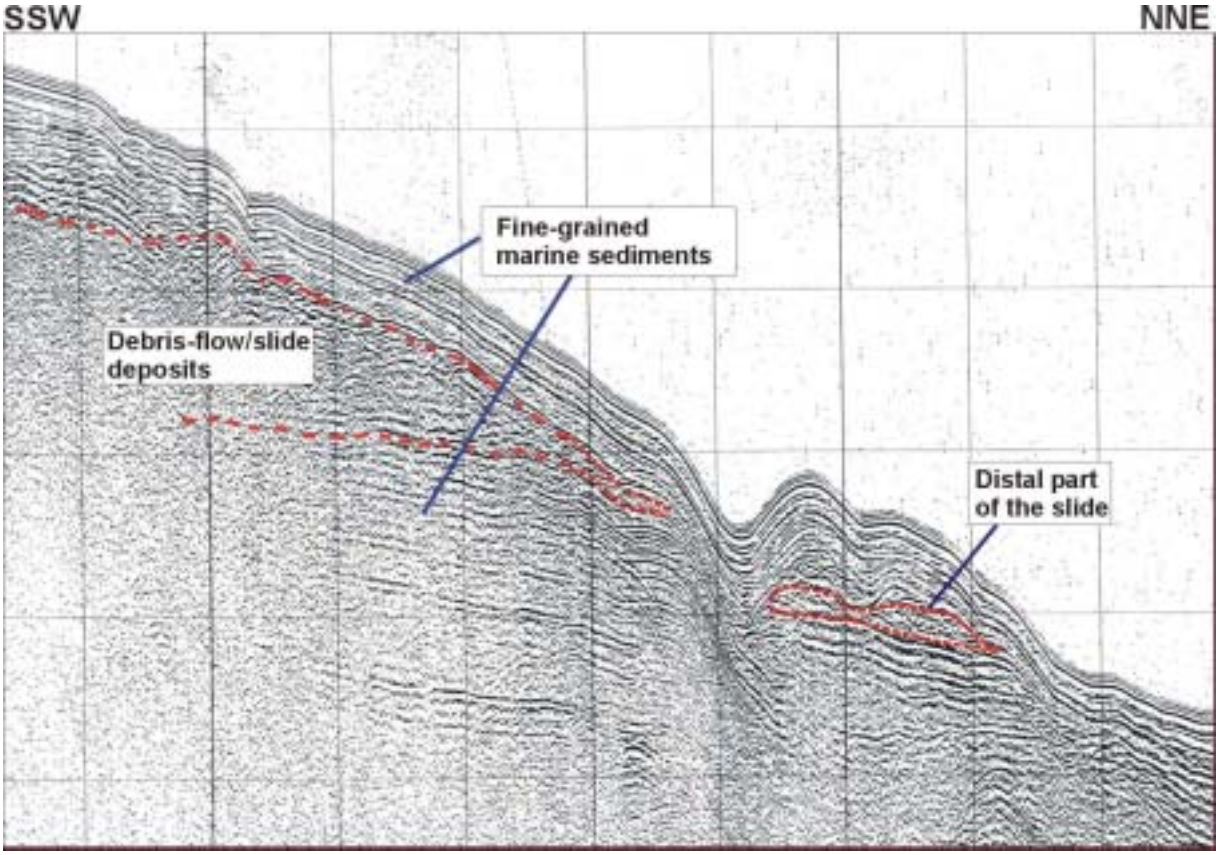

Figure 35A. Seismic profile from the northernmost part of the studied fjord area (profile A in Fig. 34).

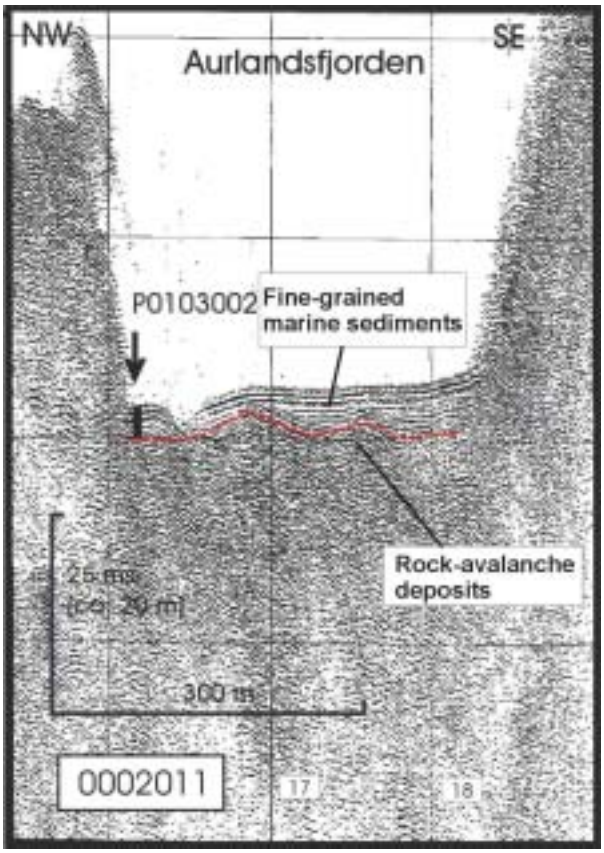

Figure 35B. Seismic profile B, shown on Fig. 34. The locality of the core presented in Fig. 36 is shown.

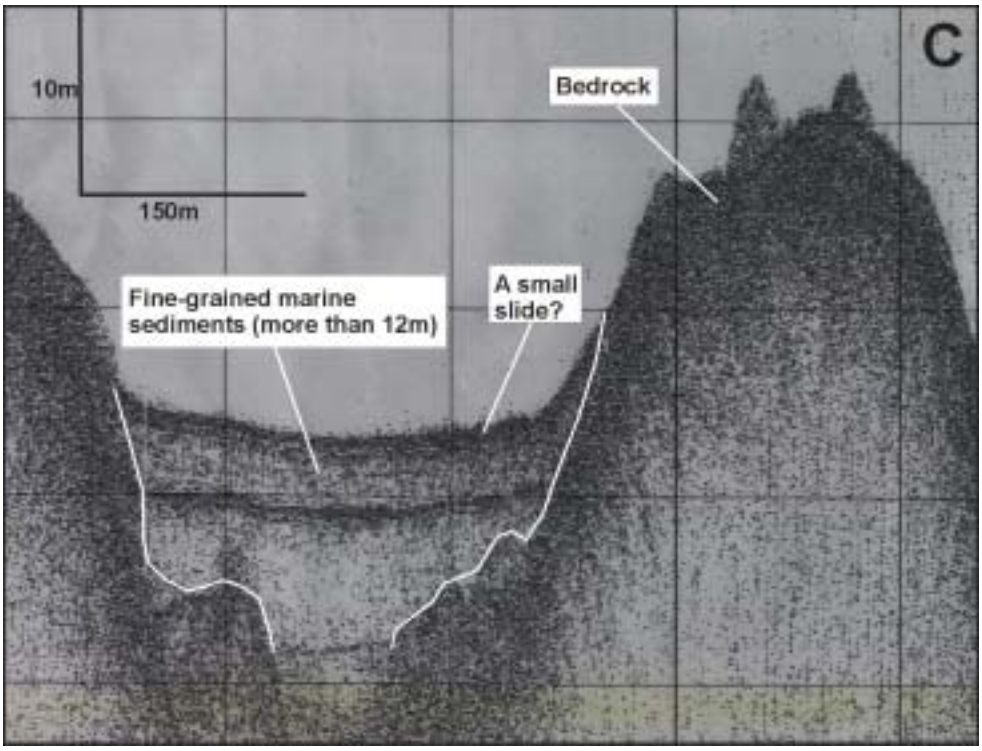

Figure 35C. Seismic profile C is from a local basin between bedrock ridges (profile C in Fig. 34).

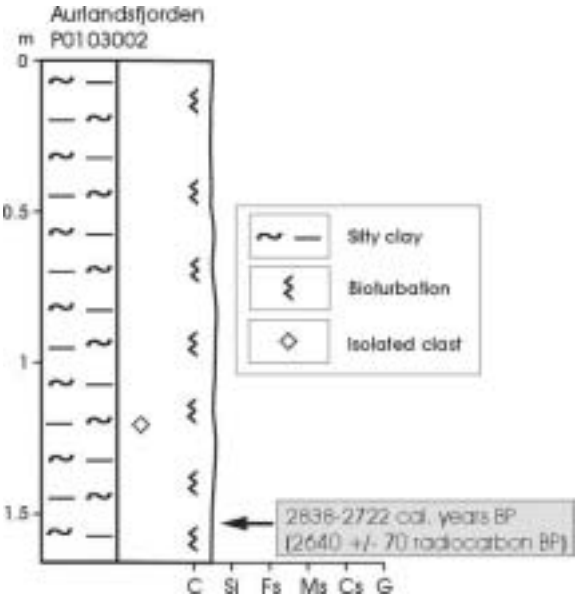

Figure 36. A core from Aurlandsfjorden (from Lepland *et al*., 2002), se locality in Fig. 35B.

3.3.2 Fjærland

Several rock- avalanche deposits have been mapped on land, close to Fjærland, and a seismic survey has demonstrated a series of rock-avalanches in the fjord. The largest was triggered in the Berrføttene area, were a large and well-defined slide scar occurs in the mountain side. The seismic data show that the avalanche crossed the fjord. Laterally, it can be traced about 4 km to the SW. Several cores were taken in order to date some of the events, but three samples for dating were barren (Lepland *et al*., 2002). A rock avalanche on the delta in the inner part of

Fjærlandsfjorden is probably younger than 1000 years with basis in interpretation of georadar data (Lauritsen & Elvebakk, 2001).

4. Post-glacial faults in Innfjorden

Geological studies in northern Fennoscandia have documented several postglacial faults, proving that this region has experienced some major earthquakes and local surface deformation (e.g. Kujansuu, 1964; Lundquist & Lagerbäck, 1976; Olesen, 1988; Dehls *et al*., 2000B). However, during the review and revisiting of existing neotectonic claims, most reported in the literature, by the NEONOR project (Neotectonics in Norway), it was demonstrated that only the two postglacial faults evidenced in Troms and Finnmark can be classified as almost certainly related to neotectonics (Olesen *et al*., 2000; Dehls *et al*., 2000A). Many of the other claims are most easily explained as gravity-driven collapse. All the reports assessing possible postglacial deformation within southern Norway could be explained by gravitational or erosional processes (Olesen, op cit). The Berill fault, a newly discovered structure in northern W Norway, is described here. It is situated in a zone characterised by a cluster of rock-avalanche events (Anda *et al*., 2002).

4.1 Berill post-glacial fault

The prominent fracture-lineament, here named the Berill fault (Fig. 37), were first observed from helicopter, and from aerial photographs during a reconnaissance study in this distinct rock- avalanche zone (Anda *et al*., 2002). The structure were then fieldchecked; its relationship to the Quaternary features, and the geomorphic evolution of the area, has been studied and evaluated. The lineament is c. 2 km long with an up to 5-6 m high escarpment trending N-S. It can be traced from about 400 m asl close to the valley floor, upslope across the relatively steep mountain side, and crossed the mountain ridge ca 1200 m asl. Downwards to a small glacier (Fig. 38). The fault defines a relatively straight line, but makes a small sideway jump at ca. 700 m asl. The total displacement when taking the slope gradient into account, is thought to be in the range of 2-4 m. The structure cuts through glacial-till surfaces in the lowermost part, and truncates avalanche-dominated colluvial fans higher on the slope, as is clearly evidenced by its relationship to the geomorphic features (Figs. 37 & 38). The glacial till, and especially the colluvial fan situated at ca. 700 m asl, is clearly offset by several meters along the fault (Figs. 37, 38 & 39). The colluvial fan at this location is interpreted to be formed by snow-avalanche processes, as is also evidenced by recent processes. However, there is little evidence that snow avalanches after the actual faulting has modified the fault scarp significantly (Fig. 39). This imply that the faulting event could be relatively young, and at least happened after the cold, Younger Dryas period, during which small glaciers occupied the small cirques in the area. At this time the snow-avalanche activity were significantly higher than today (Blikra & Nemec, 1998). The sediment transport from the glaciers, and the snow avalanches, would certainly have modified and destroyed the fault scarp during this period. The fault scarp is well exposed in bedrock higher on the slope; it is moderately ($\approx 45^{o}$) W-dipping and associated with rockfall processes (Fig. 40). Fault breccias have been observed. In summary, the neotectonic Berill fault is a reverse fault that truncates Younger Dryas sediments.

A series of crevasses or fractures occur on the western, hangingwall side of the fault (Fig. 38). They are 600-800 m long and all ends in the fault zone (Fig. 40). Except for a few fractures in the southernmost part, they all trend SW-NE and are, thus, oriented oblique to the fault zone (Fig. 38). Some of the structures also controls the colluvial sedimentation by acting as traps for debris transported by snow avalanches (Fig. 41). The southern part of the mountain slope west of the Berill fault shows indications for gravitational sliding and may be

termed a rock-slide feature (Figs. 38 & 42). Some open fractures in the south-western part are oriented 90º to the fault (Fig. 42), but this is most probably controlled by gravitational movements of the entire mountain slope in this area (see map in Fig. 40).
The Berill fault cannot be interpreted as a gravitational feature due to its prominent linear trend and the way it crosses the mountain ridge. Reverse separation is another strong argument for regional tectonic forces. Fractures are strictly found in the hangingwall of the fault. The described structure is interpreted to be a reverse, up-to-the-E fault, with a displacement of 2-4 m. The fault is the first clear evidence of postglacial faulting in southern Norway. Observations of a similar lineament further south, hints at a possible continuation of the Berill fault.

4.2 Age of the fault

The Berill fault is younger than the Younger Dryas period (13.000-11.500 cal. years BP), and the moderate modification of the fault scarp may indicate that the faulting occurred during the second half of the Holocene. The Berill fault occurs in an area characterised by a high number of rock-avalanche events (Fig. 43). A series of rock avalanches and fractures have been mapped in the nearby Romsdalen valley, 15-20 km to the east. At least 4 large rock avalanches occur 4-6 km down-valley from the Berill area, and at least one of them triggered a major, secondary debrisflow, which descended several kilometres down the valley. Excavations and dating of organic material from these sediments demonstrated that the event was at least younger than 3800 cal. years BP. Furthermore, there are historical indications of a large rock-avalanche event in the year 1611 AD. In this case, with a documented neotectonic fault, it is reasonable to believe that the high number of rock-avalanche events in this region are controlled and triggered by relatively young seismic activity. This implies that large earthquakes and local surface deformation can occur today, possibly triggering failures both on land and in the fjords. One feasible interpretation is that postglacial faulting in this region not were connected to the time shortly after the deglaciation, nor to the period with highest land uplift. This area (Innfjorden) is actually situated to a zone with one of the largest gradients of the present land uplift in western Norway (Dehls *et al*., 2000A).
Further detailed investigation of the Berill fault is recommended. Studies should include trenching through the fault, in order to (i) gather material for dating faulting activity and (ii) judge weather the fault moved in one or multiple seismic events. The latter will shed light on the size of the earthquake(s). Studies of the fault zone in bedrock may yield valuable results on fault-zone characteristics and displacement direction, which can be applied to other areas.

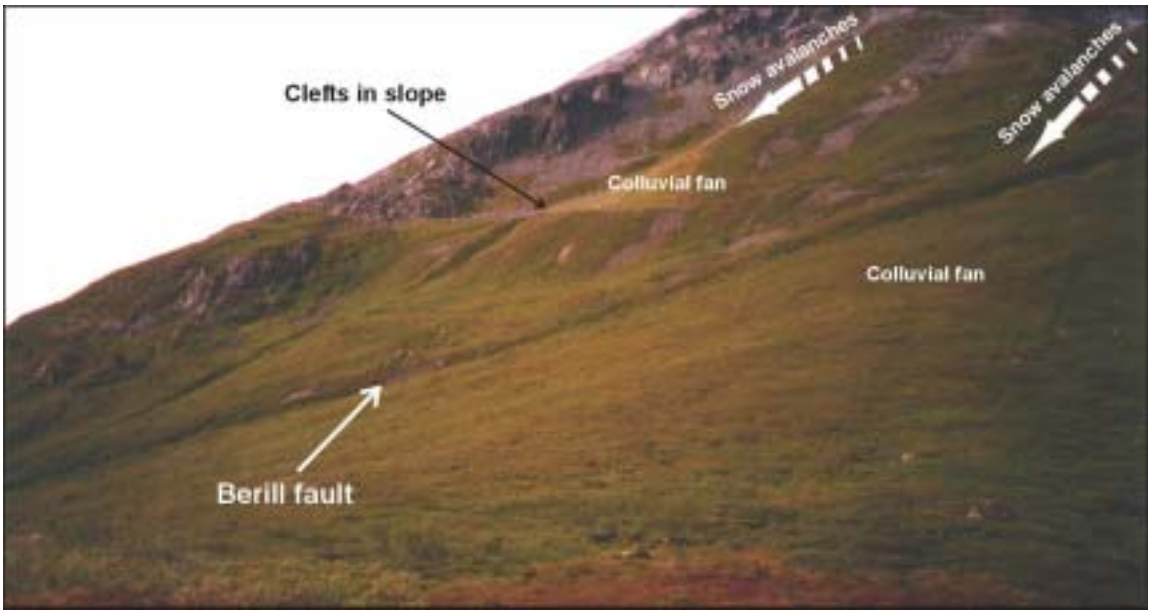

Figure 37. The prominent lineament interpreted to be a postglacial fault, the Berill fault. Note that the fault clearly truncates the colluvial fan and displaces it several meters (up to the right).

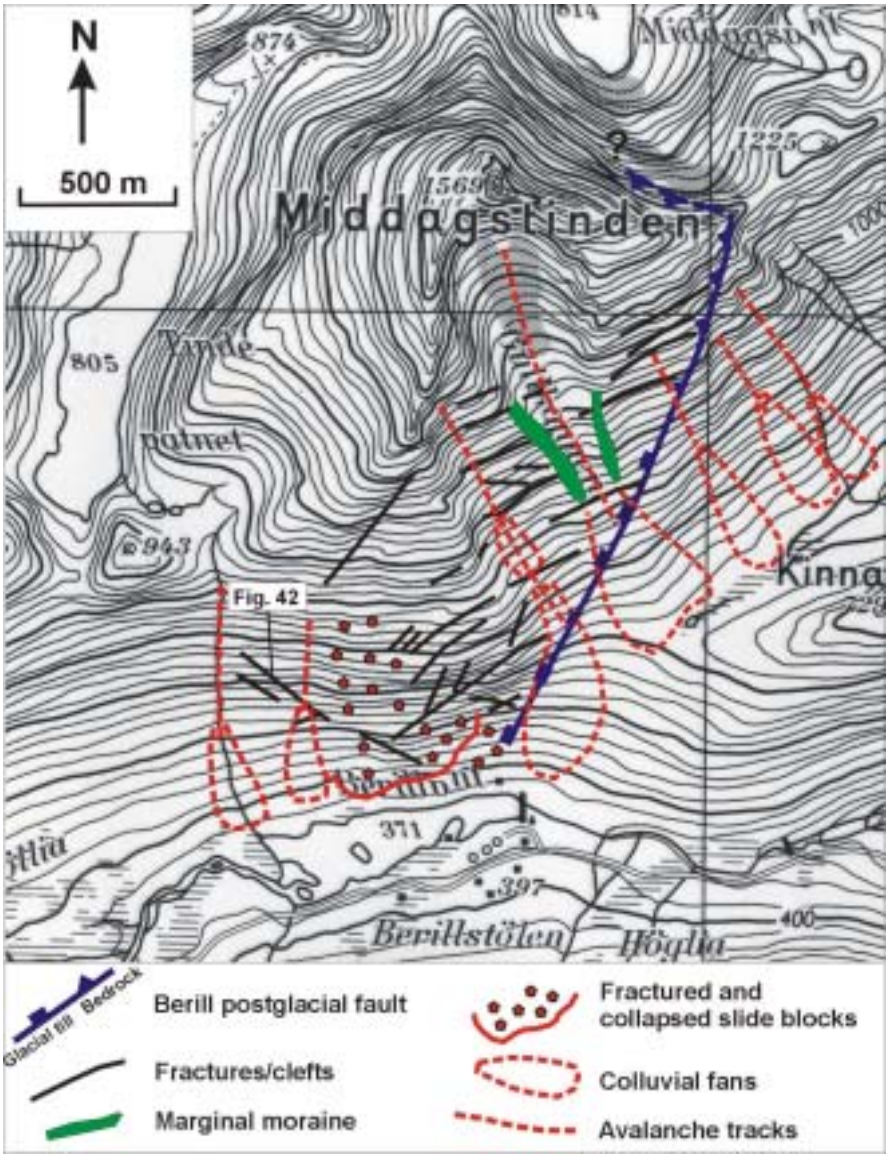

Fig. 38. Map showing the Berill fault, fractures and clefts and the main Quaternary geomorphic elements. The fault strikes approximately N-S and dips moderately W.

Figure 39. Details of the Berill fault were the fault cut into a colluvial fan. There are no indications of later modification by creep or avalanche processes.

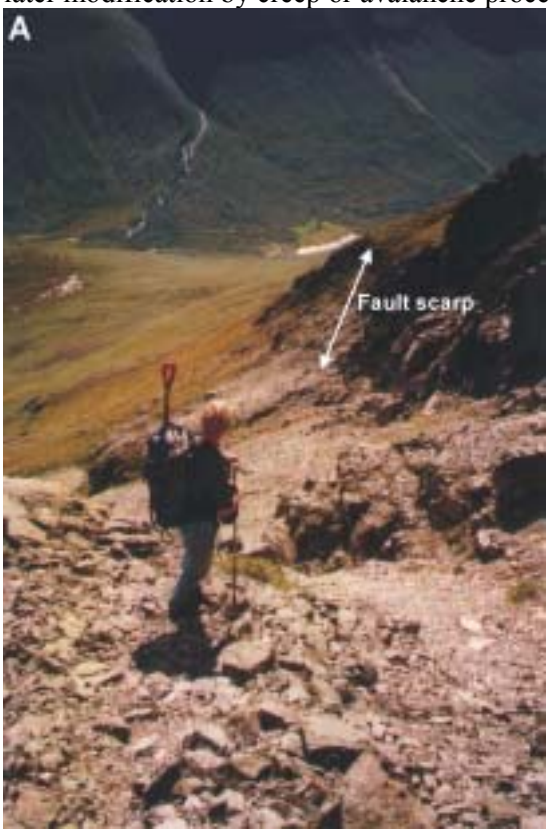

Figure 40. The Berill fault is well exposed in bedrock high on the mountain slope. The fault scarp is unstable, as documented by minor rock falls.

Figure 41. Fracture cutting into glacial debris and colluvial fans on the western side of the fault zone. The cleft ends in the fault. Note that the cleft act as a sedimentation trap for deposits transported by recent snow-avalanches

Figure 42. Open fractures further west. The cleft is situated in a collapsed part of the mountain slope (see locality in Fig. 38). View is to the SE.

5. Regional distribution and timing of events

Geological mapping on land and in the fjords in Møre & Romsdal has identified a series of rock-avalanche events throughout the last 15 000 years. The geographic distribution shows a clustering in specific zones (Fig. 43). More than 100 individual events larger than 1 mill. m^3 have been located, with the largest avalanche estimated to have a volume of about 100 mill. m^3, in Tafjorden. The rock-avalanche events are not yet systematically registered in Sogn & Fjordane, and the data presented are only preliminary.

5.1 Regional distribution

Geological studies confirm that several zones have been affected by a significant number of large rock avalanches throughout the postglacial period (Blikra *et al*., 1999), as displayed in Fig. 43. The distribution of rock-avalanches clearly demonstrates that the frequency of events is highest in the inner fjord areas. However, one concentration is found around Oterøya and another further to the southwest. A database containing historical avalanche events, including snow avalanches and debrisflows, is under construction at NGU in close coorporation with Astor Furseth (Nordal commune in Møre & Romsdal). These data clearly show the high number of rock-avalanche events in the inner fjord areas. The largest events in the fjord areas have triggered tsunamis, which are shown in Fig. 44. All events with registration of tsunamis are found in the inner fjord areas, except for the Tjelle event in Langfjorden (historical slide in 1756).

From the data on geologically mapped rock-avalanche events (Fig. 43) and the historical events (Fig. 44) it can be concluded that the high-risk areas are in the inner fjords of western Norway (Fig. 26). No historical events are recorded from the Oterøya, Vanylven and Ørsta areas (Fig. 44). This suggests that the events in the coastal areas (Fig. 43) may be relatively old (just after the deglaciation), or alternatively, are very rare events. The possibility that large earthquake(s) have played a role cannot be excluded. Actually, the geographic concentration of rock avalanches hints at a common triggering mechanisms, e.g. one or more earthquakes.

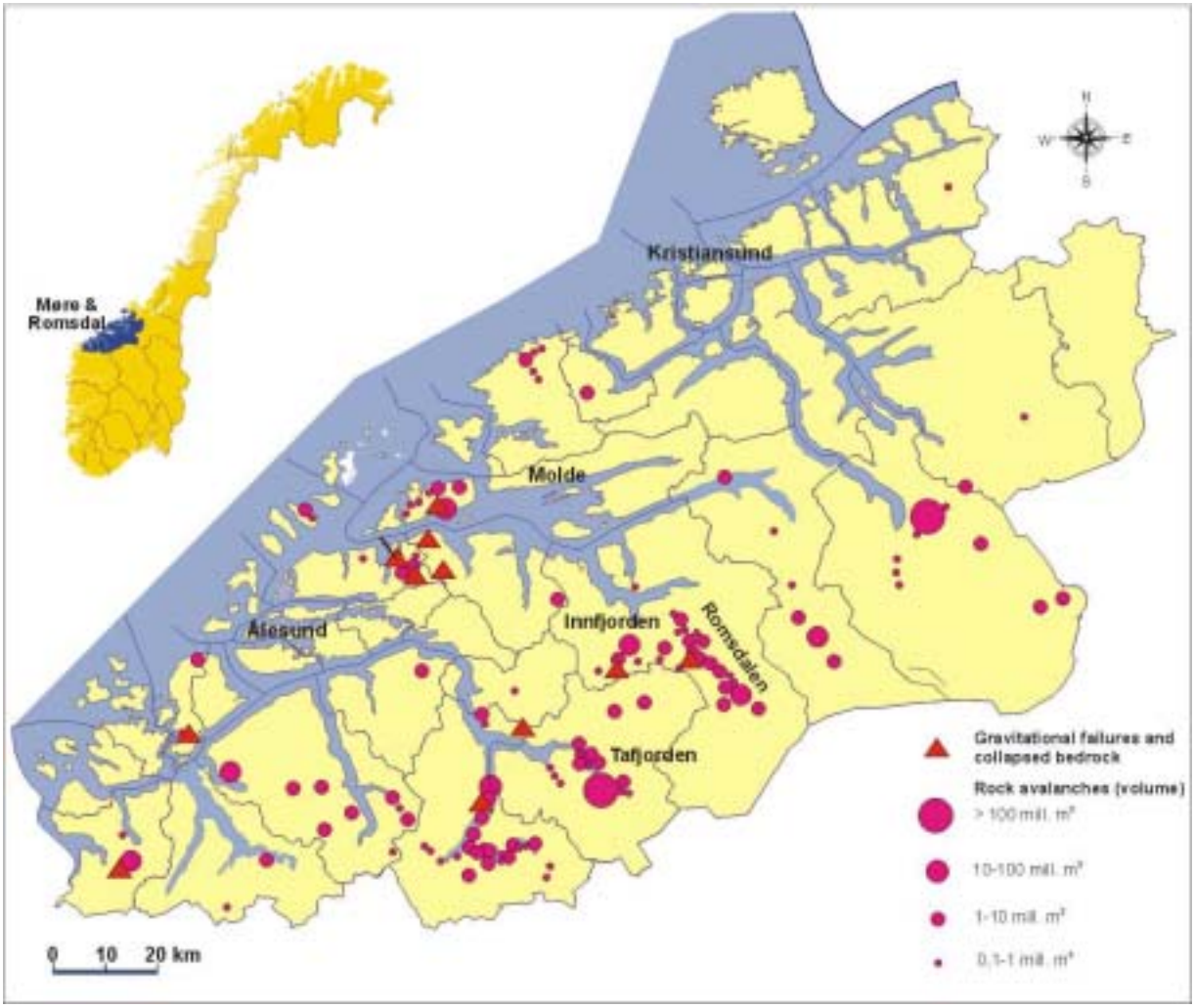

Figure 43. Registration of rock-avalanche events and gravitational fractures in Møre & Romsdal county.

In Sogn & Fjordane, a total review and systematic registration of all gravitational-slope failures has not yet been executed. However, a reconnaissance study based on interpretations of aerial photographs in a 20 km wide zone from Odda in Hardanger to Aurland in Sogn has been carried out by Blikra *et al*. (2000A). This demonstrates more than 20 areas of gravitational faults and/or large rock avalanches (Fig. 45). These occur along a SSW-NNE trend from Odda to Aurland, and include the gravitational fractures and rock avalanches described from Flåmsdalen and Aurlandsfjorden. Other areas of many rock-avalanche events in Sogn & Fjordane is Nærøyfjorden (west of Aurlandsfjorden), Fjærlandsfjorden and the inner fjord system of Sognefjorden (Lusterfjorden – Fortun), see indicated areas in Fig. 46. Furthermore, a series of rock avalanches are found in the inner Nordfjord area.

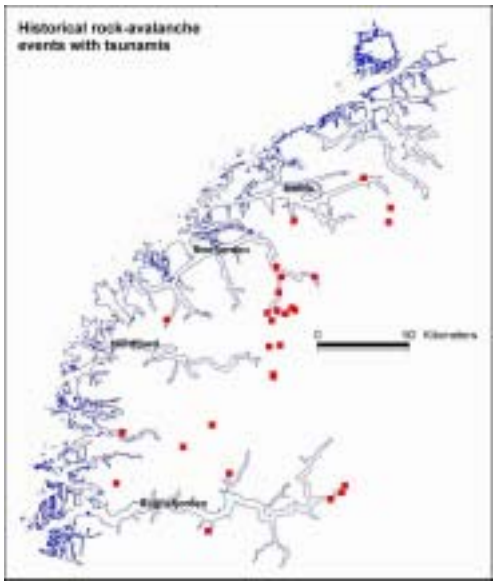

Figure 44. Historical rock-avalanche events with related tsunamis in Møre & Romsdal and Sogn & Fjordane. Source: historical database (NGU/Astor Furseth).

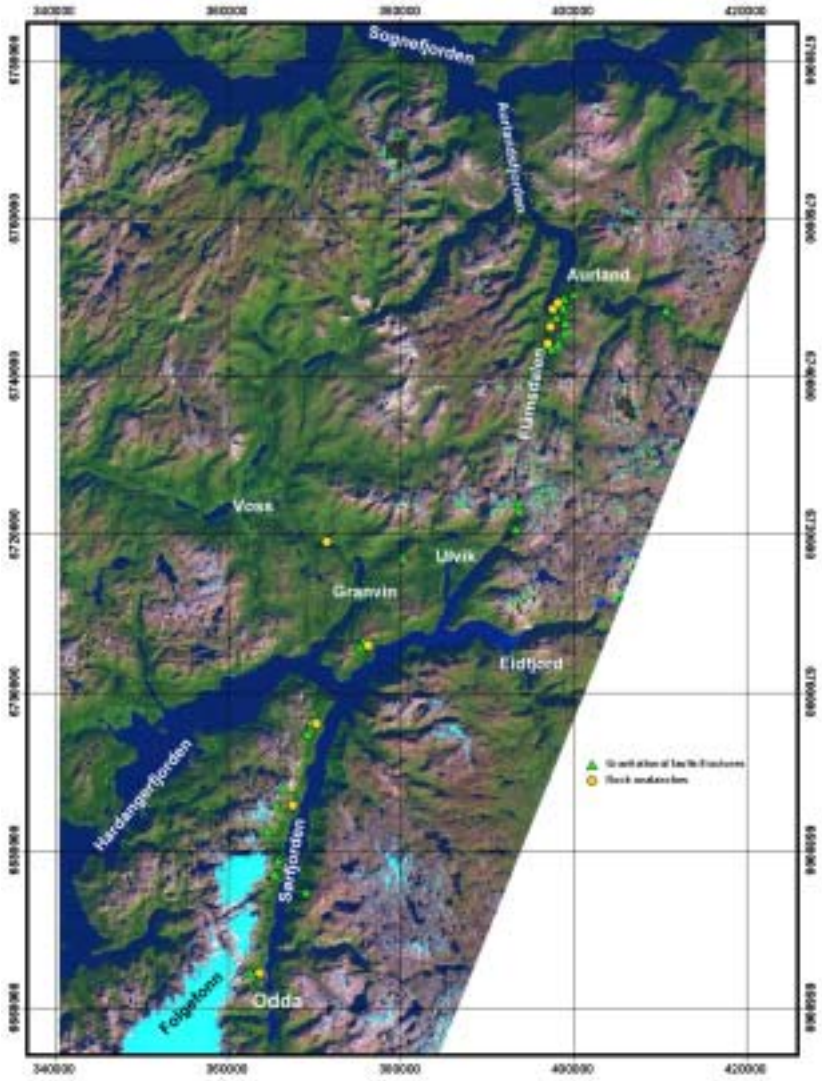

Figure 45. Satellite image showing locations of gravitational-slope failures in an area from Odda in Hardanger to Aurland in Sogn. An interpretation of aerial photographs has been conducted in a 20 km wide area from Odda to Aurland. The line spacing is 20 km. From Blikra *et al*. (2000A).

5.2 Age

Events which have been either directly dated by the radiocarbon method or indirectly dated by use of seismic stratigraphy or sea-level curves are listed in Table 1. This shows that many are from the latest part of the postglacial period (the last 5000 years).

The suggested old age of the fractures and rock avalanches on Øtrefjellet indicates that the instability features there occurred shortly after the deglaciation (15-14 000 cal. BP). The fractures and rock avalanches in the Ørsta, Syvdsfjorden and Hareid area suggest both old and young ages (Table 1). The time constraint is weak, although ages >11 500 cal. BP in Ørsta and Hareid and <11 500 cal. BP in Sørdalen in Syvdsfjorden, are suggested. This points to several events of different ages. A series of dates in the inner fjord areas suggests high rock-avalanche activity during the second half of the Holocene (Table 1). Furthermore, several dates around 3000 BP may suggest some kind of relationship with the Berill neotectonic fault in Innfjorden.

The data from Aurlandsfjorden suggest that the largest rock avalanche there occurred shortly after the deglaciation (11 000-10 000 cal. years BP; Table 1), and that it might be related to the formation of the gravitational faults in the area. A younger and smaller event occurred in Aurlandsfjorden at about 3000 cal. years BP.

Table 1. Dated rock-avalanche deposits in Møre & Romsdal and Sogn & Fjordane counties. Historical events are not listed.

Locality	Age (Cal years BP)	Dating method	Dated material	Reference
Venje, Romsdalen	<1400 BP	^{14}C	Charcoal	
Hole, Romsdalen	<4000 BP	Sea level		
Myra, Romsdalen	>5800 BP	^{14}C	Peat	
Remmem, Romsdalen	>2300 BP	^{14}C	Peat	
Innfjorden	<3800 BP	^{14}C	Palaeosols	
Tafjord I	<3100 BP	^{14}C	Foraminifera	Lepland *et al*., 2002
Tafjord II	>5000 BP	Seismic stratigraphy		
Hareid	>11500 BP	Sea level (Younger Dryas frost-shattering)		
Skorgeura, Ørsta	>11500 BP	Sea level (Younger Dryas frost-shattering)		Blikra, 1994
Øtrefjellet	>11500 BP	Vedde ash layer		
Sørdalen, Syvdsfjorden	<11500 BP	Sea level		
Oldedalen	6000 BP	^{14}C	Tree log	Nesje, 2002
Fjærland	<1500 BP	Sea level		Lauritsen & Elvebakk, 2001
Aurland I	c. 10-11000 BP	Seismic stratigraphy		Blikra *et al*., 2001
Aurland II	c. 3000 BP	^{14}C	Foraminifera	Lepland *et al*., 2002

6. Trigger mechanisms

Triggering mechanisms for large rock avalanches in the region are poorly understood, but extreme rainfall building up high water pressure in fractures, and high-amplitude earthquakes are probably the most important factors. Increased movement, seen as widening of clefts, have been observed for quite long periods before rock-avalanche events (e.g. Tjelle, Tafjord and Loen slides). This suggests that gravitational creep can be active for long periods, and the failure itself do not necessarily need to be controlled by earthquake or rainfall events.

6.1 Creep caused by increased water pressure and weathering

Creep is a relatively slow process that in many cases seems to occur prior to rock-avalanches, as hinted at above. This is well illustrated by a disastrous avalanche in Italy (Erismann & Abele 2001), which caused collapse of a hydropower dam and thereby flooding of a populated valley. During filling of the dam, creep was recorded along one of the slopes of the dam margin. With increased water level, i.e. increased pore pressure in the rock, creep accelerated. Because of this, the filling of the dam was stopped, resulting in diminishing creep that gradually was reduced to zero. At this stage it was concluded that the unstable area had stabilised, and filling of the dam was sustained. Some hours later, the entire unstable area avalanched into the dam. This suggests that, in this case, initial creep resulted in strain softening of the basal shear layer, hence reducing the critical basal shear strength.

In order to trigger creep for an unstable area, the total forces acting on the basal sliding surface have to overcome the critical friction force. Two common mechanisms for reduced friction, acting either isolated or in symphony, are; (I) increased pore fluid/water pressure along the shear surface, and (II) weathering of the shear surface. It is important to keep in mind that these processes are time dependent; hence stability evaluations for a given time are temporally unreliable.
Case I: Increased water pressure reduces the normal stress on the shear plane, thereby reducing the shear strength. Creep in this context means that sliding starts at a critical value of pore pressure, and that the pressure immediately drops below the critical value when movement takes place. Hence, captured pore pressure is released during microscopic slip events, which appear repeatedly. If the pressure is preserved, or increased, rather than released, the slip event will develop and accelerate, and likely evolve into a full-scale rock avalanche, unless some mechanism blocks the development, for example an obstacle at the toe of the sliding rock body.
Case II: Weathering of the basal shear plane can be viewed along two lines: (a) Mechanical and/or chemical breakdown of microscopic obstacles which are stress localisers on the surface. Thereby, the smoothness of the plane is enhanced, commonly resulting in reduced friction. (b) Chemical alteration of fractured and damaged minerals at or near the shear surface that, for example, may result in formation of new clay minerals. Such minerals can lubricate the shear plane, and therefore reduce the shear strength.

In all cases, as soon as a critical shear value is reached, movement will accelerate unless other factors act in the opposite direction. Accelerating movement results in destruction of minerals or clasts at the basal shear surface, which then develop into a soft layer of crushed rock (gouge and breccia), lubricating the shear surface and reducing the shear strength, i.e., a strain softening process. Development of a gouge zone, and especially if it becomes continuous, dramatically reduces the stability of a collapsing area.

Creep process is thus an important factor for triggering of rock avalanches, and as an example, the Oppstadhornet failure is interpreted to be affected by such processes (see Blikra *et al*., 2001). This conclusion agrees with that of Harbitz (2002). In these reports it is argued that, if the slide was triggered off in one event and then slid down several 10s of metres, it would evolve into a full-scale avalanche.

6.2 Earthquakes

6.2.1 Earthquake triggering of rock avalanches

According to the reviews by Keefer (1984) and Jibson (1994), triggering of large rock avalanches requires a minimum earthquake magnitude of about 6.0. Furthermore, Jibson (*op.cit.*) concluded that large rock avalanches are the type of avalanche activity with greatest potential in palaeoseismic studies. Deep, coherent slides in bedrock (rock slumps and rock-block slides), seem to require even stronger earthquakes (M 6.5; see Keefer, 1984).
The earthquake distribution recorded from year 1750 to 1999 in southern Norway shows that the area with the highest earthquake activity is found off and along the western coast of Norway (see review by Dehls *et al.* 2000A), as shown in Fig. 46. Earthquakes of magnitude 6 or higher have never been recorded in Norway.
Review of historical and recent data on seismically induced landslides shows that the full range of landslide types can be initiated by seismic activity, and 81% of all slope failures occurred in the region with mean horizontal peak ground acceleration (PGA) greater than 1.5 m/s^2 (Sitar & Kahazai, 2001). A PGA of 1.5 m/s^2 is comparable to an earthquake with magnitude somewhat above M 6 within a distance of 20-30 km. Seismic-hazard analysis for Norwegian onshore and offshore areas shows that large areas of the northern part of western Norway is situated within PGA values of more than 1.5 m/s^2 for an annual probability of 10^{-3} (NORSAR & NGI, 1998). If this model is reliable, earthquake-triggered landslides should be found in western Norway.

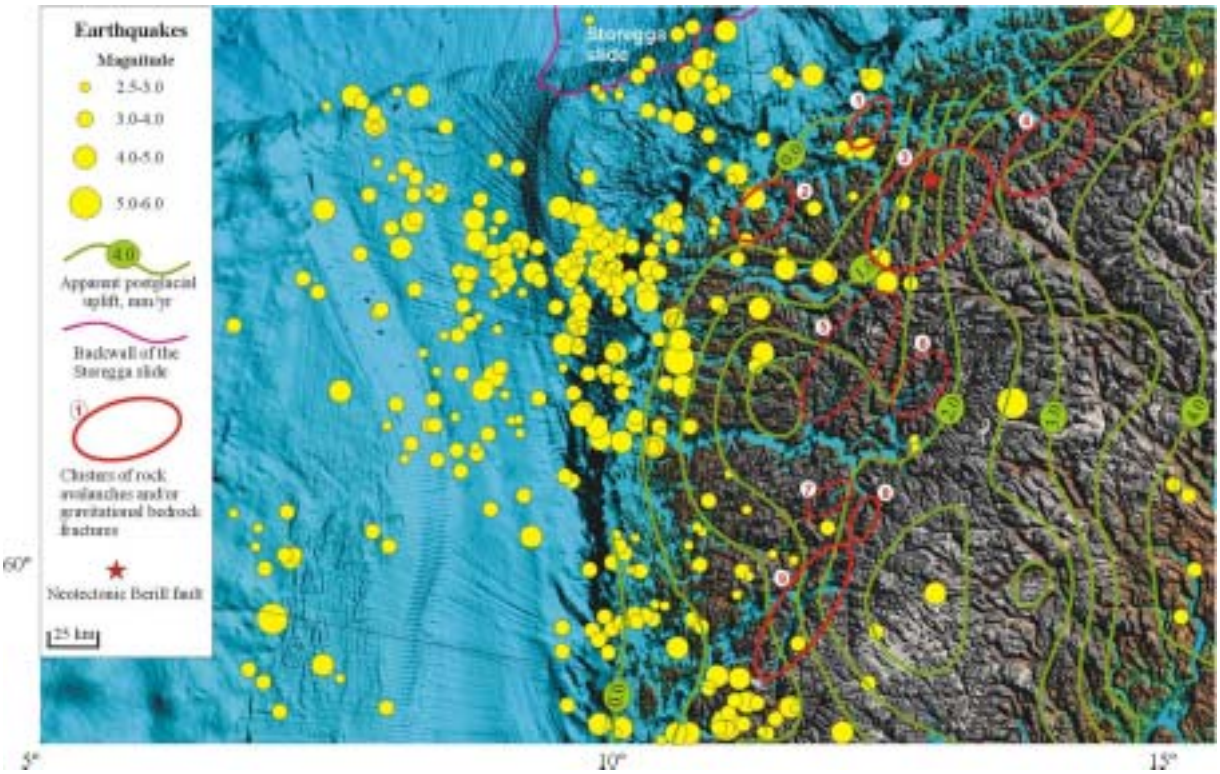

Figure 46. Earthquake data (NORSAR) and apparent land uplift plotted on a Landsat 7 satellite image base (modified from Dehls. *et al*., 2000A). Areas with high frequency of rock avalanches and gravitational bedrock fractures, and the neotectonic Berill fault (Anda *et al*., 2002), are shown. Investigations are not finished in the stippled areas. The numbered areas are: (1) Oterøya - Øtrefjellet; (2) Vanylven - Ørsta; (3) Tafjord – Innfjorden - Romsdalen; (4) Eikesdalen - Sunndalen; (5) Nordfjord area; (6) Lusterfjorden area; (7) Nærøyfjorden; (8) Aurlandsfjorden - Flåmsdalen; (9) Hardangerfjorden.

6.2.2 Structural geology and uplift data

Fig. 46 shows earthquake data and apparent land uplift (NORSAR) plotted on a Landsat 7 satellite image base. A lineament map (NGU's structural database) is plotted together with the earthquake data and the satellite image in Fig. 47. Most earthquakes are found offshore northern West Norway. Although there is no evidence of any connection, most earthquakes are found where the NE-SW striking Møre-Trøndelag Fault Complex intersects the N-S trending Øygarden fault zone. There, a limited number of earthquakes have been of magnitude 5 to 6. It is worth to mention that only a few earthquakes are recorded along the Møre-Trøndelag fault complex. This major fault zone is likely dominated by creep (Pascal & Gabrielsen 2001), hence, there is an open question weather or not sufficient build-up of stress may occur on the zone. However, if the fault complex periodically locks, significant earthquake swarms can be expected.

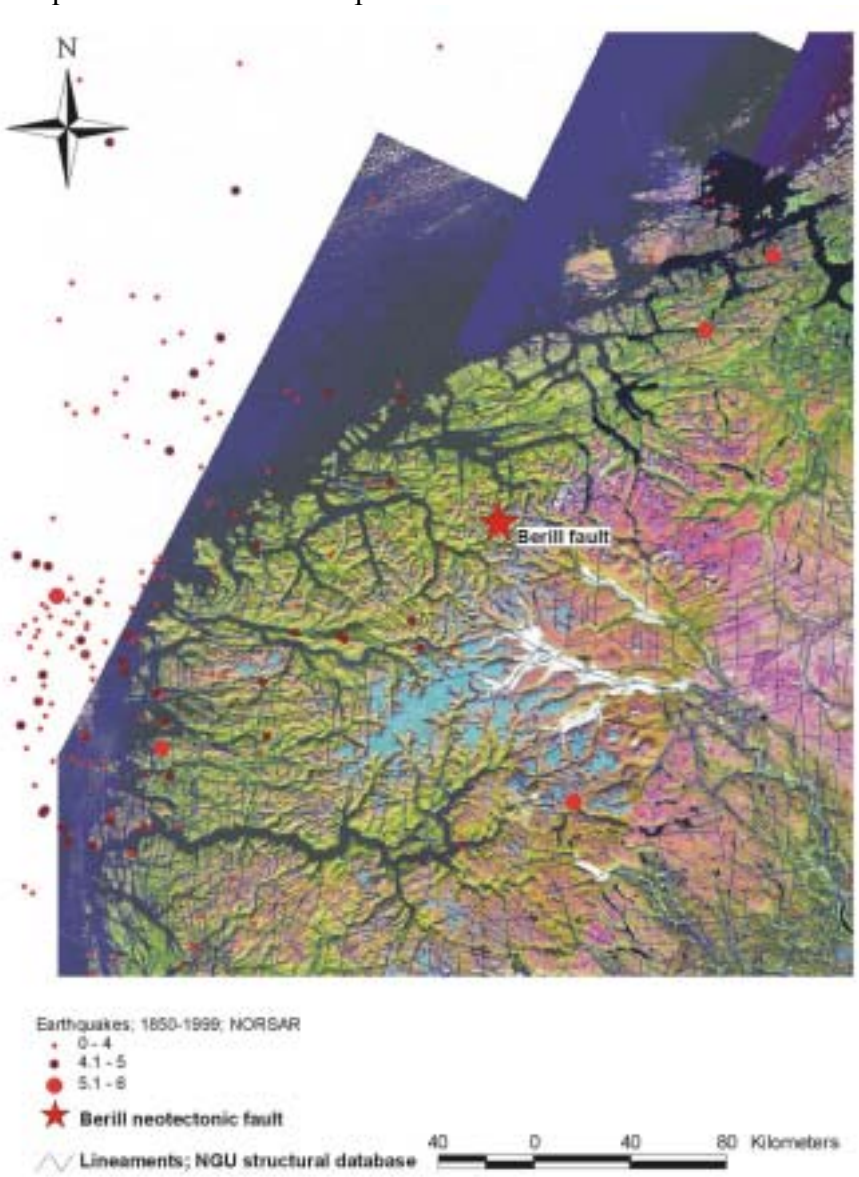

Figure 47. Earthquake (NORSAR) data plotted on the lineament map with a Landsat 7 satellite image base (NGUs structural database).

The recently detected neotectonic fault ca. 50 km SSE of Molde (Berill fault, Anda *et al*., 2002) may help to explain some rock avalanches in this region (Fig. 46), however, the earthquake database does not reveal recent neotectonic activity on the structure. Strikingly, the Berill fault is situated in the area of the highest gradient of land uplift in western Norway (Fig. 46).

6.2.3 Area of instability features and earthquake magnitude

It is known, from studies of historical earthquakes, that these may trigger debris and rock failures (Keefer 1984; Jibson 1994). The spatial occurrence of such events and their age relationship can thus be used for palaeoseismic analysis. The relationship between earthquake magnitude and area affected by landslides has been analysed by Keefer (1984), see Fig. 48. If an area of 500 km^2 was influenced by mass-movements during an earthquake, this would imply a magnitude of M = 5.7-6.2. The area affected by slides is often found as an ellipse (Adams, 1981). Keefer also examined the relationship between the magnitude and maximum distance of landslides from epicentre and fault rupture (Figs. 49 & 50).

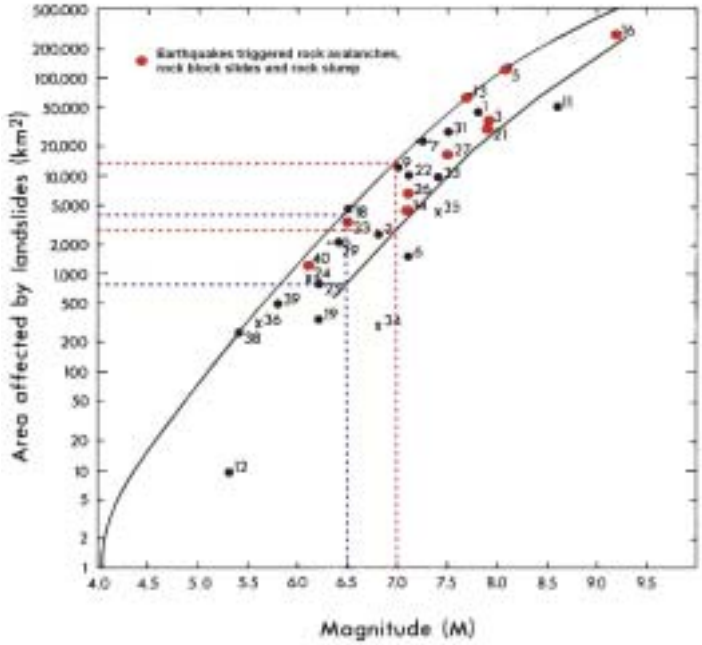

Figure 48. Area affected by landslides in earthquakes of different magnitudes (after Keefer, 1984). Events triggering rock avalanches, rock-block slides, and rock slumps, are shown in red. Areas affected by landslides during earthquakes of 6.5 and 7.0 are indicated. An earthquake of M 6.5 would for example imply an area affected by landslides of between 800 and 4000 km^2.

The main areas of rock avalanches and gravitational bedrock fractures are shown together with the Berill fault on Fig. 46. The coastal areas at Oterøya and Øtrefjellet are about 25 km long and 15 km wide. The areas are then about 300-350 km^2, and this would then imply an earthquake magnitude of 5.5-6.2 (Fig. 48). However, according to Keefer (1984), deep bedrock failures probably require an earthquake of M 6.5. The area affected by other types of mass failures should then be much larger, at least 800 km^2 (e.g. 40 km long and 25 km wide).

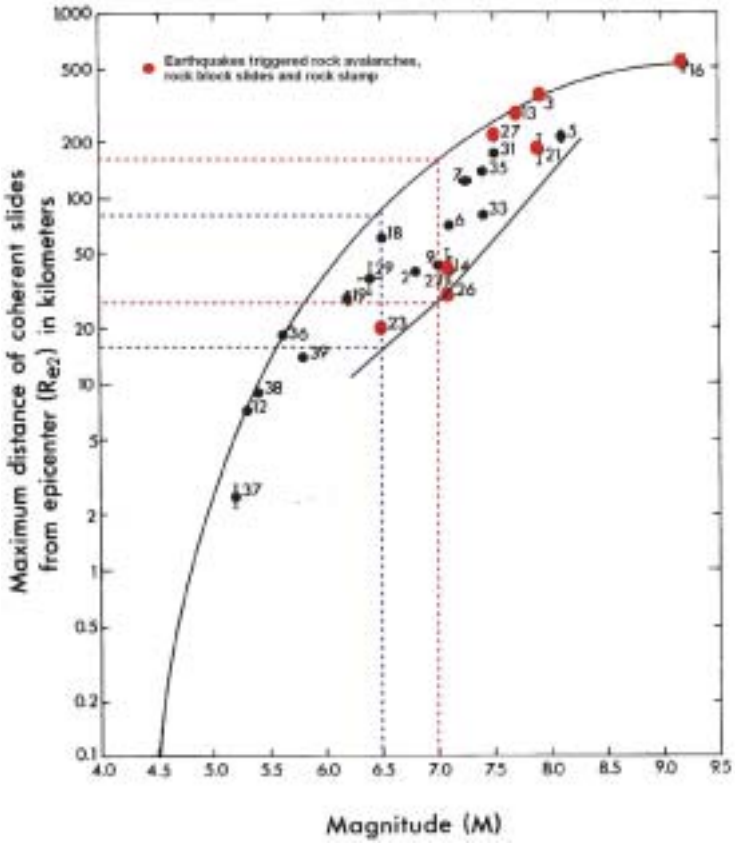

Figure 49. Maximum distance from epicentre to landslides for earthquakes of different magnitudes (after Keefer, 1984). Events triggering rock avalanches, rock-block slides, and rock slumps, are shown in red.

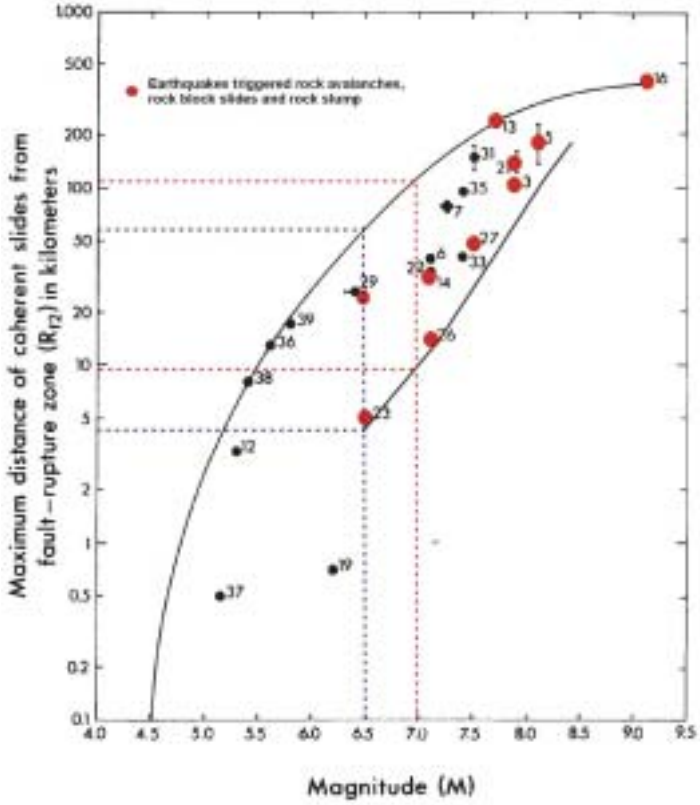

Figure 50. Maximum distance from fault-rupture zone (surface location) to landslides in earthquakes of different magnitudes (after Keefer, 1984). Events triggering rock avalanches, rock-block slides, and rock slumps, are shown in red.

The Berill fault, which is a reverse fault at least 2 km long and with throw in the range of 2-4 m, is consistent with a major seismic event, possibly in the range of magnitude 6.5 to 7.5 (Carver & McCalpin 1996). If there is a continuation of the fault towards the south, this gives a rupture length of between 10 and 15 km, indicating an earthquake in the range of magnitude 6.5 to 7.0 (Anda *et al*., 2002.). Alternatively, the offset could relate to multiple, smaller events. An earthquake of M 6.5 would imply that an area of 800 to 4000 km^2 was affected by slides (40-90 km long and 25-50 km wide, see Fig. 48). This area is indicated on Fig. 51 and seems to correlate well with the aerial extent of the observed slide clusters (Fig. 46). If we use the relationship between magnitude and rupture, an earthquake of M = 6.5 would imply slides up to 60 km away, whereas a conservative estimate is up to 20 km from the rupture (Fig. 50). If we use the relationship between the epicentre and landslide occurrence, landslides may occur up to 80 km away (Fig. 49).
If earthquakes of magnitude M = 7.0 have occurred in this region, an area of 3000 – 12 000 km^2 should bee affected by slides (e.g. 75-150 km long and 45-90 km wide, see Fig. 48). Such areas are indicated in Fig. 51. Areas potentially affected by slides of earthquakes of M = 6.5 and 7.0 are also indicated with centre in the Oterøya-Øtrefjellet cluster (Fig. 51).

The geographic distribution of rock avalanches and gravitational bedrock fractures shows a quite good fit with what should be expected by earthquakes of magnitude M = 6.5 (Figs. 46 and 51). Earthquakes of M = 7,0 would probably affected larger areas. It is, however, important to relate these data to the distribution of other types of mass movements, e.g. subaqueous slides in the fjords.

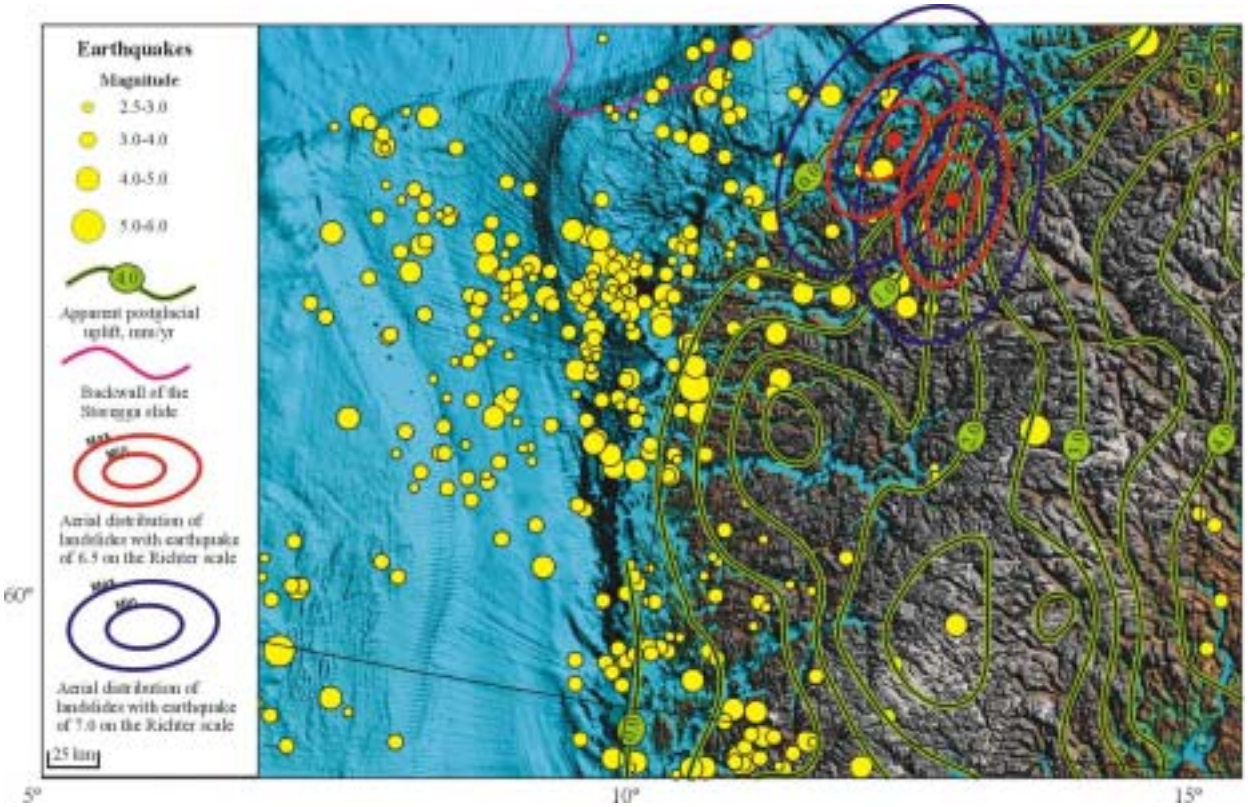

Figure 51. Earthquake data (NORSAR) and apparent land uplift plotted on a Landsat 7 satellite image base (modified from Dehls *et al*., 2000A). Aerial distribution of potential landslides during earthquake events of magnitude 6.5 and 7.0 in area 1 and 3, shown in figure 46, is indicated. Potential areas affected by landslides are derived from the relationship found by Keefer (1984, see Fig. 48).

7. Conclusion

Geological studies show that several areas in western Norway have been affected by a significant number of large rock avalanches throughout the postglacial period. The geographic distribution of rock avalanches and gravitational bedrock failures clearly show a clustering in specific zones, with the highest frequency in the inner fjord areas of western Norway. The highest number of such features is found in the Romsdalen and Tafjord areas in Møre og Romsdal. Clusters of rock-avalanche deposits and gravitational bedrock fractures are also found in two smaller areas of the coastal part of Møre og Romsdal, around Oterøya and Syvdsfjorden. Many gravitational failures also occur in the phyllite areas in Aurland, Sogn og Fjordane.

It is known from studies of the effects of historical earthquakes that these may trigger various types of debris and rock failures. The spatial occurrence and dating of individual events can thus be used for palaeoseismic analysis. Review of historical earthquakes indicate that the triggering of large rock avalanches requires a minimum earthquake magnitude of about 6.0 on the Richter scale, and large rock avalanches are probably the type of mass movement with the greatest potential in palaeoseismic studies. Deeper-seated bedrock failures require probably even higher magnitude earthquakes in order to be triggered, probably of the order of M 6.5. The distinct clustering of features in specific zones indicate that large earthquakes may have played a triggering role.

The temporal control is still weak in most areas, but a review of existing data has been conducted. The well-defined clustering of bedrock fractures and rock avalanches around Oterøya occurred probably shortly after the deglaciation (15-14 000 cal. BP). The time constraint is weak for the coastal area further southwest (Ørsta, Syvdsfjorden and Hareid), although ages >11 500 BP in Ørsta and Hareid, and <11 500 BP in Sørdalen in Syvdsfjorden are suggested. This points to several events with different ages. A series of ages from the inner fjord areas of Møre og Romsdal suggest high rock-avalanche activity during the second half of the Holocene. Furthermore, a neotectonic fault (Berill fault) in Innfjorden, ca. 50 km SSE of Molde, west of Romsdalen, is documented in this area. The Berill fault is at least younger than the Younger Dryas period (<11 500 BP). Some dated rock avalanches around 3000 BP, in Innfjorden and Tafjorden, may suggest a relationship with the movement(s) on the Berill fault. The data from Aurland, in Sogn og Fjordane, suggest that the largest rock avalanche occurred shortly after the deglaciation (11 000-10 000 years before present). A younger and smaller event occurred in Aurlandsfjorden at about 3000 years BP.

The Berill fault may help to explain some rock avalanches in the inner fjord areas of Møre og Romsdal. The fault is situated to the area of the highest land uplift gradient in western Norway, which may explain possible crustal instability. Earthquake(s) related to this fault were probably of the order of M 6.5. The aerial distribution of the observed clusters seems to fit with existing data on the relationship between aerial extent of landslides and earthquake magnitudes of M 6.5. The area of bedrock fractures and rock avalanches around Oterøya may relate to an earthquake of M 6.5 shortly after the deglaciation.

An earthquake of magnitude 7.0 or larger would probably have affected vast areas of western Norway. No such event is mirrored on land, in postglacial time. We strongly recommend further investigations of possible neotectonic faults, in order to get a better understanding of the palaeoseismic activity. This is crucial for regional risk evaluation related to earthquakes and rock avalanches onshore.

8. References

Adams, J. 1981: Earthquake-dammed lakes in New Zealand. *Geology* 9, 215-219.

Anda, E. & Blikra, L.H. 1998: Rock-avalanche hazard in Møre & Romsdal, western Norway. *Norwegian Geotechnical Institute* Publication 203, 53-57.

Anda, E., Blikra, L.H. & Longva, O. 2000: Large-scale slope failures in Møre and Romsdal - Palaeoseismic evidence? 20-25 In: Dehls, J & Olesen, O. (Red): Neotectonics in Norway, Annual Technical Report. *NGU Report 2000.01*.).

Anda, E., Blikra, L.H. & Braathen, A. 2002: The Berill fault – first evidence of neotectonic faulting in southern Norway. *Norsk Geologisk Tidsskrift* in press.

Blikra, L.H. 1999: Rock avalanches, gravitational faulting and its potential palaeoseismic cause. 88-92. In: Dehls, J & Olesen, O. (Red): Neotectonics in Norway, Annual Technical Report 1998. *NGU Report 99.007*.

Blikra, L.H. & Anda, E. 1997: Large rock avalanches in Møre og Romsdal, western Norway. *NGU Bulletin* 433, 44-45.

Blikra, L.H., Anda, E. & Longva, O. 1999: Fjellskredprosjktet i Møre og Romsdal: Status og planer. *NGU Report* 99.120, pp 21.

Blikra, L.H., Braathen, A. & Skurtveit, E. 2001: Hazard evaluation of rock avalanches; the Baraldsnes area. *NGU Report* 2001.108.

Blikra, L.H., Dehls, J. & Olesen, O. 2000A: Gravitational-slope features from Odda in Hardanger to Aurland in Sogn, western Norway. 26-30 In: Dehls, J & Olesen, O. (Red): Neotectonics in Norway, Annual Technical Report. *NGU Report 2000.01*.

Blikra, L.H. & Longva, O. 2000: Gravitational-slope failures in Troms: Indications of palaeoseismic activity? 31-40 In: Dehls, J & Olesen, O. (Red): Neotectonics in Norway, Annual Technical Report. *NGU Report 2000.01*.

Blikra , L.H., Longva, O. & Anda, E. 2000B: Large rock avalanches in western Norway. Poster report: Interpraevent, Villach, Österreich, june 2000.

Blikra, L.H. and Nemec, W. 1998: Postglacial colluvium in western Norway: depositional processes, facies and palaeoclimatic record. *Sedimentology* 45, 909-959

Blikra, L.H., Longva, O. & Sletten, K. 2000C: Palaeoseismic activity and gravitational-slope failures. 33-43. In: Olesen, O. (Red): Neotectonics in Norway, Final report. *NGU Report 2000.02*.

Blikra, L.H., Tønnesen, J.F. & Longva, O. 2002: Fjellskred og stabilitet i fyllittområder – Geologiske og geofysiske studier. *NGU Report* 2002.005.

Dehls, J., Olesen, O., Bungum, H., Hicks, E.C., Lindholm, C.D. & Riis, F. 2000A: Neotectonic map: Norway and adjacent areas. *Geological Survey of Norway*.

Dehls, J.F., Olesen, O., Olsen, L. & Blikra, L.H. 2000B: Neotectonic faulting in northern Norway; the Stuoragurra and Nordmannvikdalen faults. *Quaternary science reviews* 19, 1447-1460.

Elvebakk, H. & Blikra, L.H. 1999: Georadarundersøkelser i forbindelse med undersøkelser av fjellskred i Romsdalen, Mare og Romsdal. *Geological Survey of Norway* Report 99.025.

Erismann, T.H. & Abele, G. 2001: *Dynamics of Rockslides and Rockfalls*. Springer, 316 pp.

Furseth, A. 1985: *Dommedagsfjellet – Tafjord 1934*. Gyldendal Norsk Forlag A/S.

Harbitz, C.B. 2002: Ormen Lang – Ilandføringsalternativer. Rock slide generated tsunamis – Run-up heights at Baraldsnes and Nyhamn. *Norwegian Geotechnical Institute* Report 20001472-2.

Jibson, R.W. 1994: Using landslides for Palaeoseismic analysis. In McCalpin (ed.): *Paleosismology.* International geophysics series 62. Academic press. 397-438.

Keefer, D.K. 1984: Landslides caused by earthquakes. *Geological Society of America Bulletin* 95, 406-421.

Kujansuu, R. 1964: Nuorista sirroksista Lapissa. Summary: recent faults in Lapland. *Geologi* 16, 30-36.

Lauritsen, T. & Elvebakk, H. 2001: Georadarundersøkelser av fjellskred ved Fjærland, Sogn og Fjordane. *Geological Survey of Norway* Report 2001.004.

Lepland, A., Bøe, R., Sønstegaard, E., Haflidason, H., Hovland, C., Olsen, H. & Sandnes, R. 2002: Regional landslide occurrences and possible post-glacial earthquake activity in northwest

western Norway: Core descriptions and analytical results (Phase C). *Geological Survey of Norway* Report 2002.xxx.
Lundquist, J. & Lagerbäck, R. 1976: The Pärve Fault: A lat-glacial fault in the Precambrian of Swedish Lapland. *Geol. Fören. Stockh. Förh*. 98, 45-51.
Mauring, E., Blikra, L.H., & Tønnesen, J.F. 1997 Refraksjonsseismiske malinger i Tafjord, Møre og Romsdal. *Geological Survey of Norway* Report 97.186.
Mauring, E., Lauritsen, T. & Tønnesen, J.F. 1998: Georadarmålinger I formindelse med undersøkelser av fjellskred I Tafjord, Romsdalen, Hellesylt og Innfjorden, Møre og Romsdal. *Geological Survey of Norway* Report 98.047.
Nesje, A. 2002: A rockfall avalanche in Oldedalen, inner Nordfjord, western Norway, dated by means of a sub-avalanche *Salix* sp. Tree trunk. *Norsk Geologisk Tidsskrift* in press.
NORSAR & NGI 1998: Development of a seismic zonation for Norway. Final report for Norwegian Council for Building Standardization (NBR), march 15, 162pp.
Olesen, O. 1988: The Stuoragurra Fault, evidence of neotectonics in the Precambrian of Finnmark, northern Norway. *Norges Geologiske Tidsskrift* 68, 107-118.
Olesen, O. *et al*. 2000: Neotectonics in Norway, Final report. *Geological Survey of Norway* Report 2000.002.
Pascal, C. & Gabrielsen, R. 2001: Numerical modelling of cenozoic stress pattern in the mid-Norwegian margin and the northern North Sea. *Tectonics* 20, 585-599.
Robinson, P., Tveten, E. & Blikra, L.H. 1997: A post-glacial bedrock failure at Oppstadhornet, Oterøya, Møre og Romsdal: a potential major rock avalanche. *NGU Bulletin* 433, 46-47.
Sitar, N. & Khazai, B. 2001: *Characteristics of seismically induced landslides in recent eartquakes.* In: Int. Conf. On Landslides, Causes, Impacts and Countermeasures, Eds. M. Kühne, H.H. Einstein, E.Krauter, H. Klapperich, R. Pöttler. VGE, Davos, Switzerland.